Aalborg Universitet

Implementation of a Hydraulic Power Take-Off for wave energy applications

Ferri, Francesco; Kracht, Peter

S D W E D

STRUCTURAL DESIGN OF WAVE ENERGY DEVICES

Implementation of a Hydraulic Power Take-Off for wave energy applications

Francesco Ferri
Peter Kracht

Deliverable D4.7

AALBORG UNIVERSITY

Department of Civil Engineering

Aalborg University
Department of Civil Engineering
Structural Design of Wave Energy Devices

DCE Technical Report No. 157

Implementation of a Hydraulic Power Take-Off for wave energy applications

by

Francesco Ferri
Peter Kracht

May 2013

Scientific Publications at the Department of Civil Engineering

Technical Reports are published for timely dissemination of research results and scientific work carried out at the Department of Civil Engineering (DCE) at Aalborg University. This medium allows publication of more detailed explanations and results than typically allowed in scientific journals.

Technical Memoranda are produced to enable the preliminary dissemination of scientific work by the personnel of the DCE where such release is deemed to be appropriate. Documents of this kind may be incomplete or temporary versions of papers—or part of continuing work. This should be kept in mind when references are given to publications of this kind.

Contract Reports are produced to report scientific work carried out under contract. Publications of this kind contain confidential matter and are reserved for the sponsors and the DCE. Therefore, Contract Reports are generally not available for public circulation.

Lecture Notes contain material produced by the lecturers at the DCE for educational purposes. This may be scientific notes, lecture books, example problems or manuals for laboratory work, or computer programs developed at the DCE.

Theses are monograms or collections of papers published to report the scientific work carried out at the DCE to obtain a degree as either PhD or Doctor of Technology. The thesis is publicly available after the defence of the degree.

Latest News is published to enable rapid communication of information about scientific work carried out at the DCE. This includes the status of research projects, developments in the laboratories, information about collaborative work and recent research results.

Recent publications in the DCE Technical Report Series

Contents

1 Objectives

The main purpose of the following work is to implement a hydraulic power take-off system coupled with the dynamic model of a wave energy converter. In this work the Wavestar concept will be used without any losses of the general principle since the power take-off sub-model can be coupled with any device, if a relative motion between to body is available. The document will be divided mainly in six chapters. Chapter 3 gives a general definition of the wave energy status and problems, Chapter 4 gives an overall description of a PTO system with a closer look into the hydraulic systems, Chapter 5 describes how the system has been modeled, implemented and coupled with the WEC dynamic model (Chapter 5), Chapter 6 gives an overview of the parameter used for the simulation, i.e. wave condition, numerical solver method, hydraulic parameters, etc. Chapter 7 and Chapter 8 are ending the work showing results and giving some general conclusion of what have been simulated.

2 Nomenclature

A list of acronyms and symbols used through the document are reported below,Table 1. Beside every item a brief description is given.

Table 1: Acronyms and Symbols

Symbols and Acronyms	Description
$ACRONYMS$	
WEC	Wave Energy Converter
PTO	Power Take-Off
PEC	Primary Energy Capture
OT	Over Topping
OWC	Oscillating Water Column
HP	High Pressure attribute
LP	Low Pressure attribute
$SISO$	Single-input single output system
$FOPM$	First order process model
FC	Frequency converter
DoF	Degree of Freedom
FRF	Frequency Responce Function
irf	Impulse Responce Function
OM	Operation and Mantainance
$SYMBOLS$	
d_f	floater diameter
M	Mass Matrix
I	Moment of Inertia
$CG, [x_G, y_G, z_G]$	Center of gravity
$CB, [x_B, y_B, z_B]$	Center of buoyancy
S_{ij}	Waterplane moments
ω	Frequency, [rad/s]
η	Surface elevation
Δ	Displaced volume
ξ_i	Body displacement i-th DoF
δ_{ij}	Kroenecker delta function, 1 if i=j and 0 otherwise
ϕ_i	Velocity potential for the 6 general modes
ϕ_0	Velocity potential for the incoming wave
$F_{rad}(i\omega)$	Radiation force, frequency domain
$f_{rad}(t)$	Radiation force, time domain
$F_{ex}(i\omega)$	Excitation force, frequency domain
	Continued on next page

Symbols and Acronyms	Description
$f_{ex}(t)$	Excitation force, time domain
$F_{hy}(i\omega)$	Hydrostatic force, frequency domain
$f_{hy}(t)$	Hydrostatic force, time domain
$A(\omega)$	Added Mass matrix, [6x6]
$B(\omega)$	Radiation Damping matrix, [6x6]
C	Hydrostatic Stiffness matrix, [6x6]
a_∞	Added Mass matrix at infinite frequency, [6x6]
K_{rad}	Memory Fluid kernel function or Radiation force irf
K_{ex}	Excitation force irf
$l_{PTO}(t)$	PTO Moment Arm
F_{PTO}	PTO Feedback force
β	Fluid Bulk modulus
p_A/p_B	Actual Pressure at piston chamber A/B
V_A^0/V_B^0	Initial volume of fluid in piston chamber A/B
a_A/a_B	Piston area chamber A/B side
x	Piston Position
x_0	Initial piston position
v	Piston Velocity
θ	WEC angular displacement
$\dot{\theta}$	WEC angular velocity
$\ddot{\theta}$	WEC angular acceleration
θ_0	Initial WEC angular displacement
$q(t)$	Unspecific flow rate
q_A^{LP}/q_B^{LP}	Fluid flow rate from LP reservoir to piston chamber A/B
q_A^{HP}/q_B^{HP}	Fluid flow rate from HP reservoir to piston chamber A/B
A_{leak}	Check valve leakage area
A_{max}	Maximum check valve passage area
p_{crack}	δP at which the check valve start to open
p_{max}	δP at which the check valve start to close
C_D	Check valve coefficient of discharge
ρ	Fluid density
q_m	Motor flow rate
q_{HP}/q_{LP}	HP/LP reservoir flow rate
γ	Ratio of gas heat capacities C_p/C_v
C_p	Heat capacity for constant pressure
C_v	Heat capacity for constant volume
q_{HP}^{rf}/q_{LP}^{rf}	Flow rate across the relief valve for HP/LP reservoir

Symbols and Acronyms	Description
$p_{HP}(t)/p_{LP}(t)$	HP/LP accumlator instantaneous pressure
p_{atm}	Axtmospheric pressure
α	Motor displacement
$n(t)$	Motor rotational speed
τ_{gen}	Generator time constant
τ_m	Motor time constant
P_{el}	Power delivered to the grid
P_{acc}	Power accumulated into the HP accumulator
P_{abs}	Power harvest from the floater
P_{wave}	Power carried by the incoming wave

3 Introduction

There are several challenges in converting energy from sea waves into electricity. At least, WECs need to deliver electricity in compliance with the grid code of the specific country and they need to resist up to 20 years and extreme sea conditions. While, the last issue mainly concerns with structure and economic analysis, the former one deals with power take-off (PTO) system. For these reasons and others wave energy is still in a pre-commercialized stage even if the field started to develop itself from the 1970s, leaded by the oil crisis. Even if more than 100 concepts have been patented in the last 20 years, and only few devices have reached the pre-commercial stage, there is not a leading technology yet. Apparently, among them, no one has proven a clear and continuous working time without exception. This scenario opens the door of a wide research field, which needs to define a new technology or make the available devices suitable for the commercialization stage. As mentioned before, nowadays, a WEC should not only produce power and resist the rough environmental condition, but it is request to produce the power in compliance with the grid code. This means to be able to produce energy and on top of it help the grid when it is necessary/request. This includes helping the grid to recover a fault, send reactive power to the grid when a big machine stops to work, etc. For these reasons in the last years more people started to talk about both mechanical and electrical smoothing system. The first class includes flywheel, gas accumulator, etc. while in the second class we will start to talk about Power Electronics, or Frequency Converter system, that is the state of the art in wind energy.

The primary interest of this work is the description of the governing equations and the numerical implementation of a mechanical smoothing system coupled with an hydraulic PTO. The simulation of a physical model can be especially helpful in gaining insights to the dynamic behavior and interactions that are often not readily apparent from reading theory. To be useful, a model should be realistic and yet simple to understand and easy to manipulate; these are conflicting requirements since realistic model are seldom simple and vice-versa.

Following, the first step to take is asking oneself which is the general scope of the underling system, i.e. *are the transients important or the model should represent a steady-state behavior?*

As it will be explained in the text, the work will trace transient dynamics of the mechanical components for the selected PTO system, while neglegting electrical transient behaviors.

Why hydraulic system? There are at least three different reasons to justify the utilization of this type of system within the wave energy field:

- The wave energy density is rather high and its content is carried at low frequency, which match the field of application of hydraulic systems, where slow motions and high moments are generally used.

- Hydraulic systems are well known and robust, which can reduce the OM cost.

- Hydraulic systems can be coupled with gas accumulator in order to smooth down the incident power fluctuations.

Furthermore, hydraulic systems can be assembled with components adapted from standard commercial applications and are suitable for control implementation.

4 Power Take-Off system (PTO)

4.1 General Aspects

In the following a short introduction of the available PTO systems for wave energy converters is given followed by a specific description of the hydraulic systems. The PTO system can be defined as the chain of processes that transform the available energy at the activated body, at the reservoir, at the air chamber, etc. into electricity to be delivered to the grid. Due to the scattered distribution of WEC concepts a sharp classification of the available PTO systems is not feasible, but mainly three different classes of PTO type are used in the wave energy filed:

- Direct mechanical driven system

- Air/Water turbine system

- Hydraulic System

All of them receive high forces (up to MN) with long period (from 1-20 s) while the delivered electricity needs to fulfill the requested grid quality. Furthermore, it is important to bear in mind the severe environment conditions where the device is situated (i.e. high salinity, distance from land, high load in storm condition, water spray, slamming load, etc.). These parameters define constrains, which the PTO system need to satisfy.

4.2 Power take-off types

It is possible to define a common scheme for all the three general PTO classes, where the available energy, either kinetic or potential, is transferred from the so-called primary energy capture (PEC) object (i.e. activated body, water reservoir, etc.) into the generator, in parallel with a control scheme, and a storage system (if needed). Following a general description of the three PTO classes cited.

4.2.1 Direct mechanical driven system

This type of PTO system directly links the generator to the PEC via mechanical connectors. Mechanical connectors can be a simple mooring line, a gearbox, a pulley, a belt, and they are normally used in point absorber WECs. The electricity can be generated using a linear or rotating generator. In both cases the velocity fluctuations need to be compensated using storage and a frequency converter system. For this type of PTO the available storage system can be battery or electrochemical cells, ultracapacitor and flywheel. All of them have pros

and cons, i.e. battery has relative high energy density but short life time and not environmental friendly, while ultracapacitor has longer life horizon but higher prize. The most common example of point absorber using direct mechanical driver are the Uppsala Point Absorber and the "L10" Buoy, both using a linear generator driven by the relative velocity between the active body and a reference body, which could be bottom fixed or a reaction plate.

4.2.2 Air/Water turbine system

This type of PTO transforms the energy stored in a fluid with high potential energy into mechanical energy, using a water or air turbine. When the process fluid is water, normally the PTO is coupled with an OT WEC, where the water is collected in a floating/fixed-elevated basin using a profiled ramp, i.e. Wave Dragon and SSG. Collected water at higher quote it then funnels into a low-head turbine, i.e. Kaplan or Propeller type, and discharged. Valves are used to control the flux across the turbines. Typical available head for this type of application is ranging from few meters to half a meter, in function of the basin water level, sea state, etc. Each turbine is coupled with a rotating generator, which should be able to work at variable speed. In this system both the basin and the number of turbine are used to smooth out the produced electricity.
When the process fluid is air, then the PTO is coupled with OWC WEC, where a pressure gradient across an air turbine is transformed into mechanical energy, i.e. Limpet and Pico plant, Oceanlinx floating structure. Since the air chamber works as high pressure side for half of the wave period and as low pressure side for the rest, a distributor, or rectifying system is requested. Opposite to the water turbine where there are no new concepts, into the air turbine field, new turbine types have been developed in order to achieve higher performance within the wave energy field, i.e Wells turbines. Here the turbine is coupled with a high speed rotating generator, which should be able to work at different speeds. In this type of PTO the common way to smooth the power output is basically a combination of flywheel and frequency converter.

4.2.3 Hydraulic system

In this class of PTO a liquid vector is used to drive a rotating generator through the mean of a hydraulic motor. A hydraulic piston pressurizes the fluid, which can be either oil or water, and the potential energy is then delivered either to a hydraulic motor or water turbine and transformed into mechanical energy; which is in turn exchanged to electricity into the generator. This type of PTO fits the feature of the wave potential since is able to handle high loads with long periods and translating the information into high frequency and constant speed request by the generator side. Furthermore, it is quite a robust and well known system. Hydraulic PTO can use or not use storage system, and in both cases

the frequency converter is present. The hydraulic piston is often a double acting cylinder and a valve loop, i.e. check valves, 4-way directional valves, etc. is used to rectify the flow through the hydraulic motor. This last can be a variable or fixed volume motor or a high-head impulse water turbine, i.e. Pelton type, directly coupled with a rotating generator. A common storage system for this kind of application is a gas/spring pressurized accumulator, which can already ensure a high smoothening effect. Some of the available PTO system configuration will be described more in details in the following pages. The controllability of the system is affected by the selected configuration and not all the hydraulic PTO systems are suitable for active control. Different hydraulic PTO system configurations are used in various applications as, point absorbers (Wavestar, CPT, AquaBUOY, OPT, Wavebob), attenuators (Pelamis, Dexadevice) and terminators (Oyster).

4.3   State of the art

In this section the focus is given to a literature review about the hydraulic PTO systems. The literature concerning the hydraulic PTO is one of the most rich; especially in the last decades new model have been published using various hydraulic systems and model complexity. Due to the strong knowledge in this field in the recent year also physical model have been developed and tested, [1, 2, 3]. The most studied model present in literature is a hydraulic PTO with double acting hydraulic cylinder and high and low pressure accumulator. An auxiliary accumulator is then used to control the system feeding back energy into the hydraulic cylinder if a control law is applied. Following, a reference list of the most recent works dealing with this type of model is given [4, 5, 6, 7, 8, 9]. The fluid compressibility is included in all of them, directly or in an artificial way, except for the work carried out by Falcao. A different approach is presented by Costello [10], and Kamizuru [11], where a direct driven hydraulic motor is used, in order to remove the accumulator and control the output through the generator. In addition to the cited works [12, 13, 14] investigated the implementation of the optimal control strategy together with a hydraulic PTO system. From the above, three different configurations are defined.

4.3.1   Hydraulic PTO - Configuration 1

Figure 4.1 shows the most used hydraulic PTO configuration. The bidirectional flow from/to the hydraulic piston chambers, is rectified using both a 4-way directional valve and, more commonly, a rectifying bridge based on 4-monodirectional (check) valves. The piston, that is sketched in light gray on the draw's left side, can have two bidirectional connection or four monodirectional connection pipes. Downline of the rectification block, two lines called low (LP) and high (HP) pressure rams are connected to a hydraulic motor, which lead a generator in turn. The red line represents the HP ram and the blue line the LP ram. Moreover, each of these two lines is connected to a gas reservoir used to smooth the residual
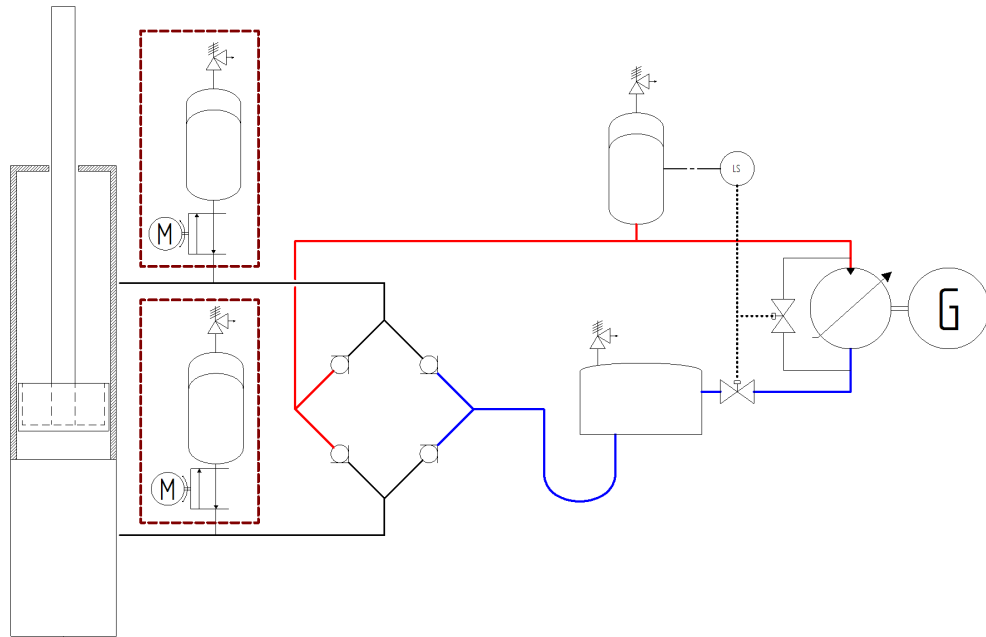
Figure 4.1: Power take-off: Configuration 1. The red identifies a high pressure ram, the blue a low pressure ram and the black both of them

pulsation coming from the rectifying bridge. This scheme is analogue to a simple diode bridge AC-DC converter, used in electronic. The motor will work only in quadrant two, which means it will sink energy only in one direction of rotation and it will not be able to feed energy back. The definition of quadrant is somehow important to define four distinct areas of operation: two directions: clockwise (CW) and couterclockwise (CCW) and two modes: acceleration and deceleration. The quadrants are defined in the torque/velocity plot. In quadrant one the system works as a motor in the CW direction, in quadrant two the system works as generator in the CW direction, in quadrant three the system works as motor in the CCW direction and in quadrant four the system works as generator in the CCW direction.

The hydraulic PTO in configuration 1 can not be controlled unless one of the following option is added:

1. Inclusion of an extra HP reservoir with controllable IN/OUT port through a 2-way

valve. Reservoirs should be connected directly to the piston chamber rams, red dotted area in Figure 4.1. The valves delay can affect the controller operation.

2. Control the flow passing through the motor with a controllable 2-way valve, which in turn controls the piston chamber pressure and therefore the feedback force of the PTO system. The inertia of the fluid can have a significan impact on the controller delay.

3. Control the flow passing through the motor adding a controllable by-pass parallel to the motor between the HP and LP rams. The accumulated energy is dissipated, that is causing a drop of performance.

The pro of this configuration is the usage of simple components, but the main drawback is the low level of control achived.

4.3.2   Hydraulic PTO - Configuration 2

Figure 4.2 represents a so called hydraulic transformer circuit scheme. As for the former case the motor is connected to the double acting hydraulic piston and the flux is previously rectified via a rectifying bridge. The motor needs to work only in the second quadrant. The hydraulic piston is decoupled from the generator side using a variable displacement pump directly connected to the shaft of the hydraulic motor. This results in a constant pressure at the generator side and the liquid can flow in a conventional fixed displacement hydraulic motor mechanically connected to a generator. Additionally, HP and LP accumulators linked to the motor rams are used to smooth any residual pressure fluctuation. The pro of configuration 3 is the absence of fluctuation in the produced electricity, but once more the main drawback is the limited control capability. As in the previous case, the introduction of extra controlled reservoirs can be used to increse the control aptitude of the system.

4.3.3   Hydraulic PTO - Configuration 3

Figure 4.3 represents a variable speed scheme. The double acting hydraulic cylinder feeds directly the motor. As a consequence of the absence of a rectifying bridge and accumulators the motor is running at varaible speed and in both direction CW and CCW. That being so the motor needs to work at least in quadrant two and four. Furthermore, if the PTO system needs to feed energy in the floater than the full four quadrants operation is needed, i.e. reactive control scheme. A relif valve is used to protect the system from high pressure levels. The pro of this system is the high controllability achived, but to avoid fluctuation in the produced energy a frequency converter needs to be included.
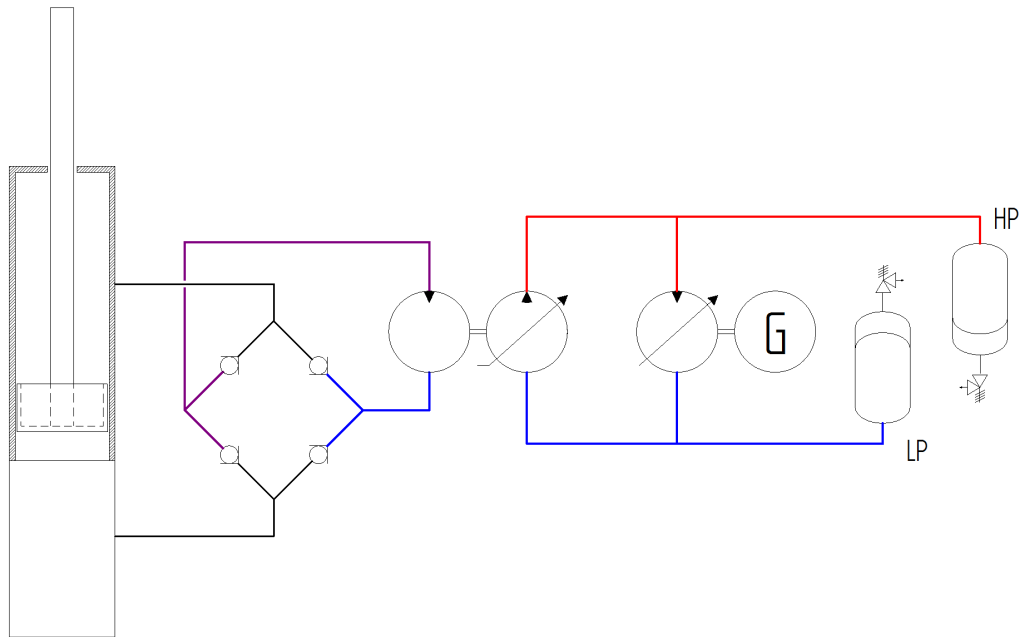
Figure 4.2: Power take-off: Configuration 2. The red identifies a high pressure ram, the blue a low pressure ram and the black a swiching pressure ram

4.3.4 Hydraulic PTO - Other configurations

The reader needs to bear in mind that this is only a rough and brief summation of the already implemented and published different concepts, and other strategy are likely to arise or been published. Just to give some examples:

- Hydraulic piston with multiple pressure chamber

- Hydraulic system with manifold and multi-level pressure accumulators

- Closed Loop Power split system with direct driven motor operating with four quadrant, high pressure reservoir and a secondary hydraulic motor with one quadrant operation

The last two PTO system are depict in the work carried-out by Kamizuru et al. [3], where it is possible to find a comparison between different PTO lay-out as a function of parameters such as controllability, limitation, adaptability, smoothness, etc (Table 4 of the above
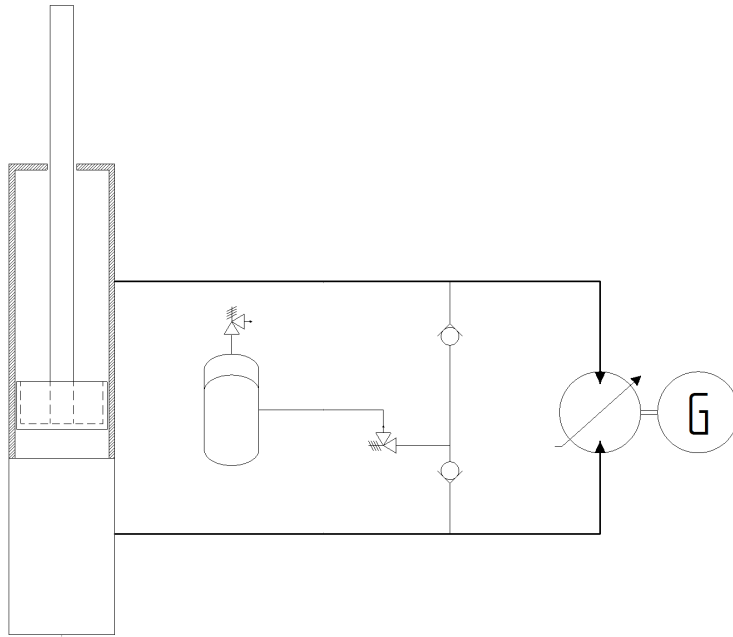
15

Figure 4.3: Power take-off: Configuration 3. The black identifies a swiching pressure ram

reference).
Once a simplified model is obtained the next step require the derivation of the governing equation and their implementation/solution using numerical methods, which will be discussed in the next chapter.

5 Model Implementation

As introduced earlier the simulation of a physical model can be especially helpful in gaining insights to the dynamic behavior and interactions that are often not readily apparent from reading theory. In this chapter the governing equations which describe the WEC and the PTO dynamic are introduced.

5.1 WEC dynamical model

The solution of the wave-body interaction can be achived with different degree of refinement. In this case a general overview or what we can call steady-state solution is sough and for this purpose the result of the Laplace equation can be searched in the form of velocity potential function, after a linearization of the boundary condition. The basic assumptions are therefore rigid body, inviscid flow, zero curl of the velocity vector field and small oscillation around the static equilibrium, which are going to restrict the results range of validity. The force acting on the system are obtained from the integration of the dynamic pressure field acting on the body wetted surface, while the pressure field can be evaluated from the velocity field obtained in turn from the velocity potential function which is solution of the Laplace equation in the fluid domain. The solution is normally obtained by splitting the problem into three different sub-problems:

- Hydrostatic problem

- Radiation problem: force induced by the motion of the body in otherwise still water

- Diffraction and Scattered problem: force induced by the wave filed with fixed structure

Holding the small amplitude assumption for incoming wave and body motion, it is possible to use the superposition principle to describe a more realistic random process. Therefore, without loss of generality it is possible to analyze the body response in regular wave, giving the chance to have a better understand of the dynamical behavior. When a regular wave is sent to the body, it will respond at the steady-state with the same frequency, while the amplitude of the response is defined by the particular geometry and applied constrains, for each of the 6 canonical modes. As shown in Figure 5.1 for a single rigid body the motion is described by three translations and three rotations relative to a global coordinate system.

Since the body response differs with the frequency it is somehow useful to define the different contributions as a frequency functions. Moreover, since the problem has been decomposed in three different linear sub-problems, each of those can be defined by a constant multiplied
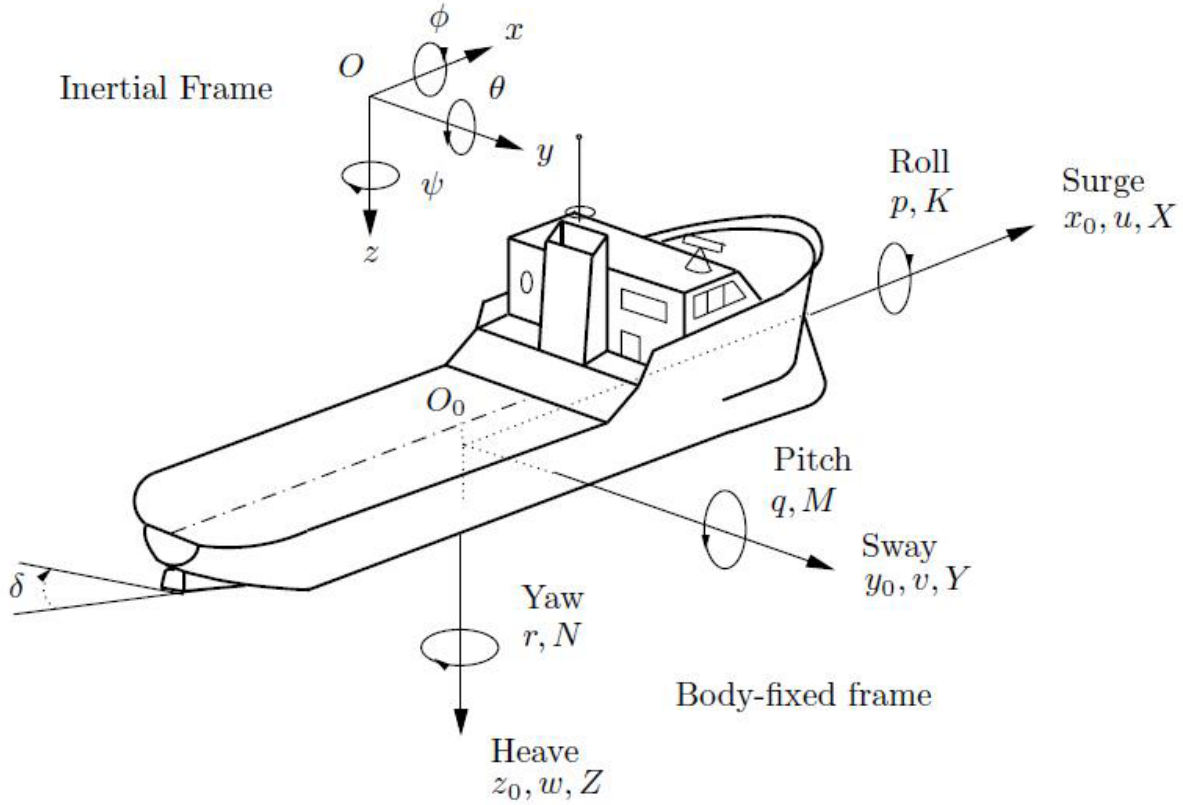
Figure 5.1: Definition of the canonical six degree of freedoms for a rigid body in water

by the specific input, for each frequency. The three different term which compose the total force are included in, eq 1

$$F_{hy}^k(i\omega) = (\rho\Delta - m)g\delta_{k2} + (mz_G - \rho\Delta z_B)g\delta_{k4} - (mx_G - \rho\Delta x_B)g\delta_{k6} - \sum_{j=1}^{6} c_{kj}\Xi_j(\omega)$$

$$F_{rad}^k(i\omega) = -\sum_{j=1}^{6}(-\omega^2\Xi_k(\omega)A_{kj} + i\omega\Xi_k(\omega)B_{kj}) \tag{1}$$

$$F_{ex}^k(i\omega) = -\rho\iint_{S_B} \left(\phi_0\frac{\partial\phi_k}{\partial n} - \phi_k\frac{\partial\phi_0}{\partial n}\right) dS = Re\{A\,mag\{F_{ex}^k\}e^{i\omega t + phase\{F_{ex}^k\}}\}$$

Where, F_{hy}^k is the hydrostatic force acting on mode k, i is the immaginary unit, ω is the rotational frequency, ρ is the water density, Δ is the volume variation, m is the mass of the system, g is the acceleration of gravity, δ_{kj} is the Kroeneker delta function, z_G is the vertical

18

position of the center of gravity, z_B is the vertical position of the center of buoyancy, x_G is the horizontal position of the center of gravity, x_B is the vertical position of the center of buoyancy, c_{kj} are the hydrostaic stiffness coefficients, F_{rad}^k is the radiation force acting on mode k, Ξ_k is Fourier tranform of the body displacement in mode k, A_{kJ} is the added mass coefficient, B_{kj} is the radiation damping coefficient, F_{ex}^k is the excitation force ancting on mode k, S_b is the wetted surface, ϕ_0 is the velocity potential of the icoming wave, ϕ_k is the velocity potential of the mode k, dS is the delta surface, A is the wave amplitude. The hydrostatic stiffness matrix (C) is constant and defined as:

$$
C = \begin{bmatrix}
0 & 0 & 0 & 0 & 0 & 0 \\
0 & \rho g S_{33} & 0 & 0 & 0 & 0 \\
0 & 0 & 0 & 0 & 0 & 0 \\
0 & 0 & 0 & \rho g S_{33} + \rho g \Delta y_B - m g y_G & -g(\rho \Delta x_B - m x_G) & 0 \\
0 & 0 & 0 & 0 & 0 & 0 \\
0 & 0 & 0 & 0 & -g(\rho \Delta z_B - m z_G) & \rho g S_{11} + \rho g \Delta y_B - m g y_G
\end{bmatrix}
$$

In order to keep the definitions as general as possible all the available DoF of the system are taken into account and therefore two index k and j running from 1 to 6 are used to keep trace of the different components; this consideration entails that the force vector will be composed by three force and three moment components, while the displacement by three translation and three rotation components. Taking the inverse Fourier transform of the above equations the different forces will be described as time functions, eq 2

$$
f_{hy}^k(t) = (\rho \Delta - m) g \delta_{k2} + (m z_G - \rho \Delta z_B) g \delta_{k4} - (m x_G - \rho \Delta x_B) g \delta_{k6} - \sum_{j=1}^{6} c_{ij} \xi_k(t)
$$

$$
f_{rad}^k(t) = \int_0^t K_{rad}^k(t-\tau)\, \dot{\xi}_k(\tau)\, d\tau \tag{2}
$$

$$
f_{ex}^k(t) = \int_{-\infty}^t K_{ex}^k(t-\tau)\, \eta(\tau)\, d\tau
$$

Where, $f_{hy}^k(t)$ is the hydrostatic force acting on mode k in time domain, ξ_k is the displacement in mode k, $f_{rad}^k(t)$ is the radiation force acting on mode k in time domain, K_{rad} is the Kernel function of the radiation force, $f_{ex}^k(t)$ is the excitation force acting on mode k in time domain, K_{ex} is the Kernel function of the excitation force and η is the surface elevation at the center of gravity of the floating body. Following, the displacement vector can be assessed solving the Newtons second law, where the system inertia is balanced by the summation of the forces acting on the system, eq. 3:

$$
F_k = \sum_{j=1}^{6} M_{kj}^{-1} \ddot{\xi}_k \tag{3}
$$

19

Where F_k is the summation of the forces acting on the body for the mode k and M is the mass matrix defined by a 6x6 matrix :

$$
M = [m_{kj}] = \begin{bmatrix}
m & 0 & 0 & 0 & mz_G & -my_G \\
0 & m & 0 & -mz_G & 0 & mx_G \\
0 & 0 & m & my_G & -mx_G & 0 \\
0 & -mz_G & my_G & I_{11} & I_{12} & I_{13} \\
mz_G & 0 & -mx_G & I_{21} & I_{22} & I_{23} \\
-my_G & mx_G & 0 & I_{31} & I_{32} & I_{33}
\end{bmatrix}
$$

Where, I_{lm} is the moment of inertia coefficient.

Plugging the time domain force decomposition described in 2 it is possible to derived what is normally known as Cummins equation, see [15].

$$
\sum_{j=1}^{6}(M_{kj} + a_\infty^k)\ddot{\xi}_k(t) + \sum_{j=1}^{6}\int_0^t K_{rad}^{kj}(t-\tau)\,\dot{\xi}_k(\tau)\,d\tau + \sum_{j=1}^{6} c_{kj}\xi_k(t) = \int_{-\infty}^{t} K_{ex}^k(t-\tau)\,\eta(\tau)\,d\tau \quad (4)
$$

Where, a_∞^k is the added mass at infinity frequency.

In addition to the hydrodynamic loads acting at the origin of the coordinate system considered it is possible to add other external forces, i.e. mooring force, PTO force, constrain forces, etc. If this extra forces are linear or can be linearized the system can be solved in frequency domain, but when non-linear forces are acting on the system the frequency domain analysis is not valid any longer and the system of equation need to be solved in time domain. The equation of motion introduced above describe the behavior of a single rigid body interacting with waves, when none of the degree of freedom is constrained. On the other hand, the WEC converter used in the simulation is a single degree of freedom system, of the point absorber type. The system is free to rotate around a pivoting point set above the water level, while all the other degree of freedoms are bounded through mechanical constrains. If those constrain are assumed to be perfect the system of equations presented in 4 simplify to a single ordinary differential equation. According to Figure 5.1 and Figure 5.2 the free mode is the number five, named Pitch. A point absorber wave energy converter has been chosen as test case, mainly for two reasons:

- Point absorbers are one of the most studied WEC systems, which means a more robust theoretical basis.

- The system is relatively easy to handle into the numerical environment, which entail a lower computational cost.

The system geometry of the Wavestar WEC is represented in Fig. 5.2. The system is not floating but hinged to a rigid structure, which stand out of the water line (corresponding to the partially sketched and cross-hatched section on Fig. 5.2). Points A and B are rotation

points connected to the structure and C is the hinge point of the PTO system relative to the lever arm, x and y define the main coordinate system and swl represents the still water level. Within the figure, only the PTO mechanical actuator is represented, corresponding to the dark gray colored item. The floater, which operates as activated body and its lever arm are represented as light grey colored items. The relative frequency response function (FRF) and impulse response function (irf) of the radiation and excitation moment as well as the mass and hydrostatic stiffness matrixes are reported in Appendix A.

Since in this case the PTO force is highly non-linear the model has been defined in time domain following the Cummins definition. The next chapter wills give an exhaustive description of the PTO model, and no further information will be added here. The numerical model of the WEC has been built using Simulink, which is a block diagram environment for multi-domain simulation and Model-Based Design integrated with Matlab. The model is presented in a multi-level sheet where sub-models, each of them defining a particular sub-system, compose the front view; the connection lines are mono directional signals carrier. The sub-system describing the WEC dynamics is reported in Appendix C.1.

5.2   Hydraulic PTO model

The hydraulic model depict in Figure 4.1 has been modeled under the following assumptions:

- No inertia and losses in fluid, pipes and valves

- No leakage in the hydraulic cylinder

- Constant bulk modulus

- Accumulator are modeled using the isentropic transformation assumption

- The dynamic of the generator and frequency converter are modeled as a first order proportional transfer function plus an inertia contribution

The above assumptions are in agreement with the one specified in the hydrodynamic model of the WEC, since the general aim is to grasp only the main dynamic of the system. Hereafter, the general equations which describe the PTO sub-model are reported, but for an exhaustive description of the hydraulic system see [16]. The first component to be modeled is the double acting hydraulic cylinder. In this case a double rod piston is used, which means a symmetric behavior of the piston in the two direction of motion. This component is the connection port between the WEC PEC and the PTO systems. The exchanged values between the two sub-systems are:

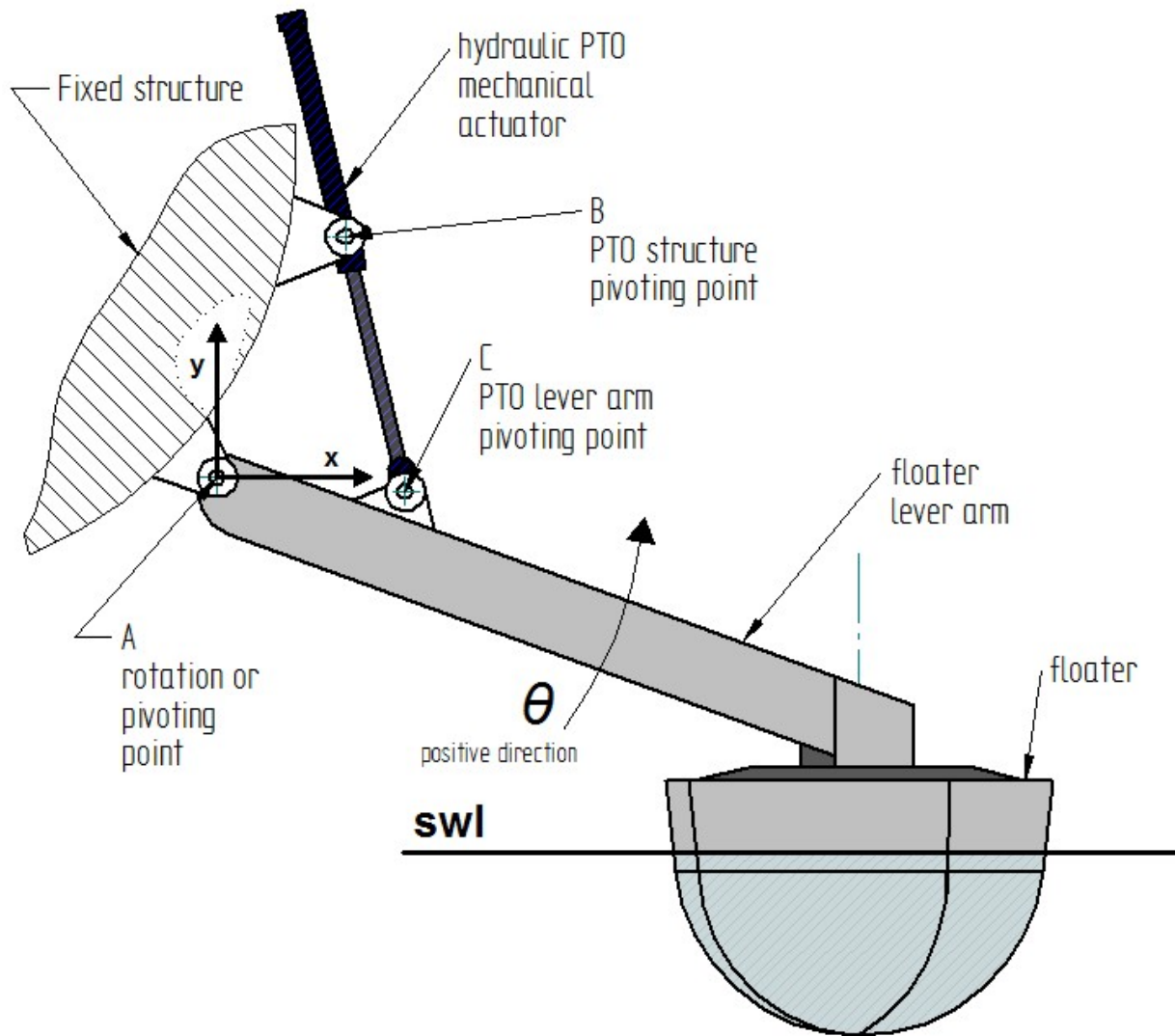$\Longrightarrow$ Piston position

Figure 5.2: Wavestar point absorber WEC

$\Longrightarrow$ Piston velocity

$\Longleftarrow$ PTO force

Where the direction of the arrows suggests the carried signals flow direction. If the arrow points to the left the information is passed from the WEC submodel to the PTO submodel, and vice-versa. In this case, since the motion of the PEC floater is described by the angular

displacement, velocity and acceleration, a conversion function needs to be defined from the geometry of the system. As it can be seen in Fig. 5.2, three rotational bearing are located in point A, B and C, and while point C is moving in time, point A and B are fixed. Therefore it is possible to calculate the angle between lines AB and AC from the actual angular displacement and its value at the equilibrium, and then solve the so called side-angle-side (SAS) triangle, for further detail see Appendix B. Knowing the length of the actuator $l_{PTO}(t)$ in function of time is then possible to obtain the bi-univocal conversion between linear and rotational motion. The mathematical model of the hydraulic cylinder is basically composed by two equations. The first describe the evolution in time of the pressure in the piston chamber, calculated from the mass balance for each them, eq 5, while the second one evaluate the PTO force applied on the PEC floater as a force balance on the piston surface, eq 6.

$$
\begin{aligned}
\frac{dp_A}{dt} &= \frac{\beta(q_A^{LP} - q_A^{HP} + a_A\,v)}{V_A^0 - a_A\,x} \\
\frac{dp_B}{dt} &= \frac{\beta(q_B^{LP} - q_B^{HP} - a_B\,v)}{V_B^0 + a_B\,x}
\end{aligned}
\tag{5}
$$

Where, p is the pressure at the hydraulic piston chamber, β is the Bulk modulus of the used fluid, q^{LP} is the fluid flow rate from the LP reservoir, q^{HP} is the fluid flow rate to the HP reservoir, a is the piston area, v is the piston velocity, V^0 is the chamber initial volume and x is the piston dispalcement. The subscript A or B indentifies the chamber A or B of the hydraulic piston.

$$
F_{PTO} = -(p_A\,a_A - p_B\,a_B)
\tag{6}
$$

Where, F_{PTO} is the PTO feedback force.

See Appendix C.2 for further details. The outgoing flux from the hydraulic piston needs to be rectified using check valves. The valves are modeled using a look-up table to relate the pressure difference between the two sides of the valve to the passage area. The piecewise function is describes by the following parameters:

- Leakage Area: Describe the leakage of the valve when the pressure across the valve is below the cracking pressure

- Maximum Area: Describe the full open valve condition

- Crack Pressure: Describe the minimum pressure at which the system start to open

- Maximum Pressure: Describe the maximum value at which the valve start to close

The flow across the valve is than calculated by eq 7

$$
q(t) = sign(\Delta p)\,A(t)\,C_D\,\sqrt{\frac{2|\Delta p(t)|}{\rho}}
\tag{7}
$$

Where, $q(t)$ is the flow rate across the valve, Δp is the pressure difference between the two sides of the valve, $A(t)$ is the area of passage of the valve and C_D is the check valve coefficient of discharge.

In this case the flow is considered to be always turbulent, therefore the low Reynold flow equation has not been used. With the same set of equation it is possible to model the relief valve for high pressure and low pressure protection. This constrain are important to keep the model as realistic as possible but still simple. For this case study these type of system protection have been oversized in order to do not overshoot the request pressure set-point. See Appendix C.3 for further details. The two accumulator (HP and LP ones) have been modeled as gas accumulator with the assumption of no volume variation of the chamber, incompressible liquid and isentropic transformation, read $pV^\gamma = const$. The actual volume of liquid available at the accumulator is calculated from the mass conservation knowing that there is only one IN port and one OUT port for the system, with their relative fluid flow rate. Following, the available volume of gas is obtained and used, holding the isentropic relation, to evaluate the pressure rate of change, eq 8

$$
\begin{aligned}
\frac{dp_{HP}}{dt} &= \frac{\beta(q_A^{LP} - q_A^{HP} + a_A\,v)}{V_A^0 - a_A\,x} \\
\frac{dp_{LP}}{dt} &= \frac{\beta(q_B^{LP} - q_B^{HP} - a_B\,v)}{V_B^0 + a_B\,x}
\end{aligned}
\tag{8}
$$

Where, p_{HP} is the pressure at the HP reservoir and p_{LP} is the pressure at the LP reservoir. An ON/OFF signal of low-low-liquid level (LLL) and high-liquid level (HL) type is sent from the HP accumulator to the motor in order to avoid the fill-up or drain-down case. See Appendix C.4 for further details. The hydraulic motor used in the model is of the fixed displacement kind. For this type of motor the torque at the shaft T_m can be calculated by eq 9

$$
T_m(t) = \lambda\,\Delta p(t)
\tag{9}
$$

Where, λ is the volumetric motor displacement. And the motor flow q_m can be calculated by eq 10

$$
q_m(t) = \lambda\,N(t)
\tag{10}
$$

Where, N is the rotational speed of the motor. The motor subsystem accepts the ON/OFF signal coming from the HP accumulator as a bang-bang controller signal. This controller acts in the following way:

- If 1 the motor torque is calculated by eq 9, the bypass valve is closed

- If 0 the bypass circuit is open with a rate limiter and the motor torque is set gradually to zero. The motor can keep on spinning and decelerate gradually.

As mentioned before the inertia of the motor has been summed to the generator one without the inclusion of any shaft stiffness. Since the motor is working only in one quadrant the rotational speed integrator carries a saturation limit to prevent negative velocity. This can be physically seen as an instantaneous check valve at the motor inlet. In this case the check valve has not been physically implemented into the model due to instability caused by the fast dynamic behavior requested. The motor does not include any damping except the emergency brake, because the generator controller was used to tune its applied torque on the system in order to match the velocity set-point.

Due to the fast dynamics of the generator and the frequency converter (FC) with respect to the motor ones, the two systems have been modeled with one single-imput-single-output (SISO) of first-order-process-model (FOPM) type, with constant time of 30ms. This approximation is possible only because the ration between the characteristic time of the generator and motor is smaller than one. The velocity controller is a simple PI controller, tuned using the marignal gain method. See Appendix C.5 for further details.

In order to analyze the different point of leakages in the transormation chains, the mean power has been calculated at three different spots: at the pivoting point (Absorbed Power, P_{abs}), at the HP accumulator (Accumulated Power, P_{acc}) and at the generator (Electrical Power, P_{el}), by (11, 12, 13)

$$P_{abs} = \frac{1}{t_{end}} \int_0^{t_{end}} \tau_{PTO}(t)\omega(t)dt \tag{11}$$

$$P_{acc} = \frac{1}{t_{end}} \int_0^{t_{end}} q_{HP}(t)p_{HP}(t) \tag{12}$$

$$P_{el} = \frac{1}{t_{end}} \int_0^{t_{end}} \tau_{gen}(t)N(t)dt \tag{13}$$

Where, t_{end} is the simulation time length, τ_{PTO} is the torque at the hinging point induced by the PTO system in the floater and τ_{gen} is the torque at the generator shaft. These quantities are then normalized by the wave power P_{wave}, calculated by (14), in order to obtain a non-dimentional system efficiency.

$$P_{wave} = \frac{\rho g^2}{64\pi}H_{m0}^2 T_p \tag{14}$$

Where, H_{m0} is the significant wave height and T_p is the peak wave period.

6 Simulations

The behavior of the integrated system, composed by the WEC model and the Hydraulic PTO model was investigated in irregular long crested waves. The water level to assess the wave body interaction is considered infinity. In particular the scatter diagram relative to Hanstholm (DK) was used, which is represented in Table 2. Table 2 report the likelihood of

Table 2: Hanstholm Scatter Diagram

$H_{m0}(m)/T_P(s)$	0.5	1.5	2.5	3.5	4.5	5.5	6.5	7.5
0.25	-	-	-	0.03	0.04	0.03	0.03	-
0.75	-	-	-	0.07	0.16	0.11	0.04	0.02
1.25	-	-	-	-	0.06	0.11	0.05	0.02
1.75	-	-	-	-	-	0.06	0.056	0.01
2.25	-	-	-	-	-	0.02	0.04	0.01
2.75	-	-	-	-	-	-	0.02	0.01
3.25	-	-	-	-	-	-	-	0.01

occurrence, on annual base, for each pair H_{m0}/T_P. For every sea state, defined by the above pair, a time series, three hours long, is generated using the white noise method [17]. The sample frequency is set to 4 Hz. In order to evaluate the annual power production the scatter diagram is then multiplied by the power production matrix, obtained from the simulations. The floater motion is not controlled and the only controllable parameter was the initial and mean pressure on the HP accumulator. The full power matrix has been assessed for five different pressure levels at the HP accumulator:

- (pressure stage 1) P1 - 10 bar

- (pressure stage 2) P2 - 50 bar

- (pressure stage 3) P3 - 100 bar

- (pressure stage 4) P4 - 150 bar

- (pressure stage 5) P5 - 200 bar

This can be seen as a slow controller for the system, which can be tuned on hour base. The PTO characteristics are recapped in Table 3

The system of equation were solved using a variable order solver based on the numerical differentiation formulas, *ode15s*. The Runge-Kutta method with order 4 showed instability and a solver for stiff problem was chosen.

26

Table 3: Hydraulic Model Parameters

Hydraulic Piston						
Υ	d_{pist}	d_{rod}	V_{dead}	β	p_0	p_{sat}
$[m]$	$[m]$	$[m]$	$[m^3]$	$[Pa]$	$[Pa]$	$[Pa]$
3	0.1	0.05	0.001	1.66e9	1e5	1e4
Check Valve and Bridge Rectifier						
C_D	ρ	A_{leak}	A_{max}	p_{crack}	p_{max}	
$[-]$	$[kg/m^3]$	$[m^2]$	$[m^2]$	$[Pa]$	$[Pa]$	
0.7	800	1e-12	0.8e-3	1e2	15e3	
Accumulators						
V	V_{HP}^0	V_{LP}^0	p_{HP}^0	p_{LP}^0	p_{max}	
$[m^3]$	$[m^3]$	$[m^3]$	$[Pa]$	$[Pa]$	$[Pa]$	
1	0.3	0.7	variable	1e5	400e5	
Motor and Generator						
α	T_k	N_{max}	J_{MG}	q_{min}		
$[m^3]$	$[N/bar]$	$[rpm]$	$[kgm^2]$	$[m^3/s]$		
3.5e-6	0.35	4250	1.5e-3	1e-9		

7 Results and Discussions

The main outcome of the simulations is reported in Fig. 7.1 and Fig. 7.2, where the annual power production and mean efficiency, in terms of electrical power, is shown as a function of the HP pressure. The subplots are related to the five pressure classes used, as reported
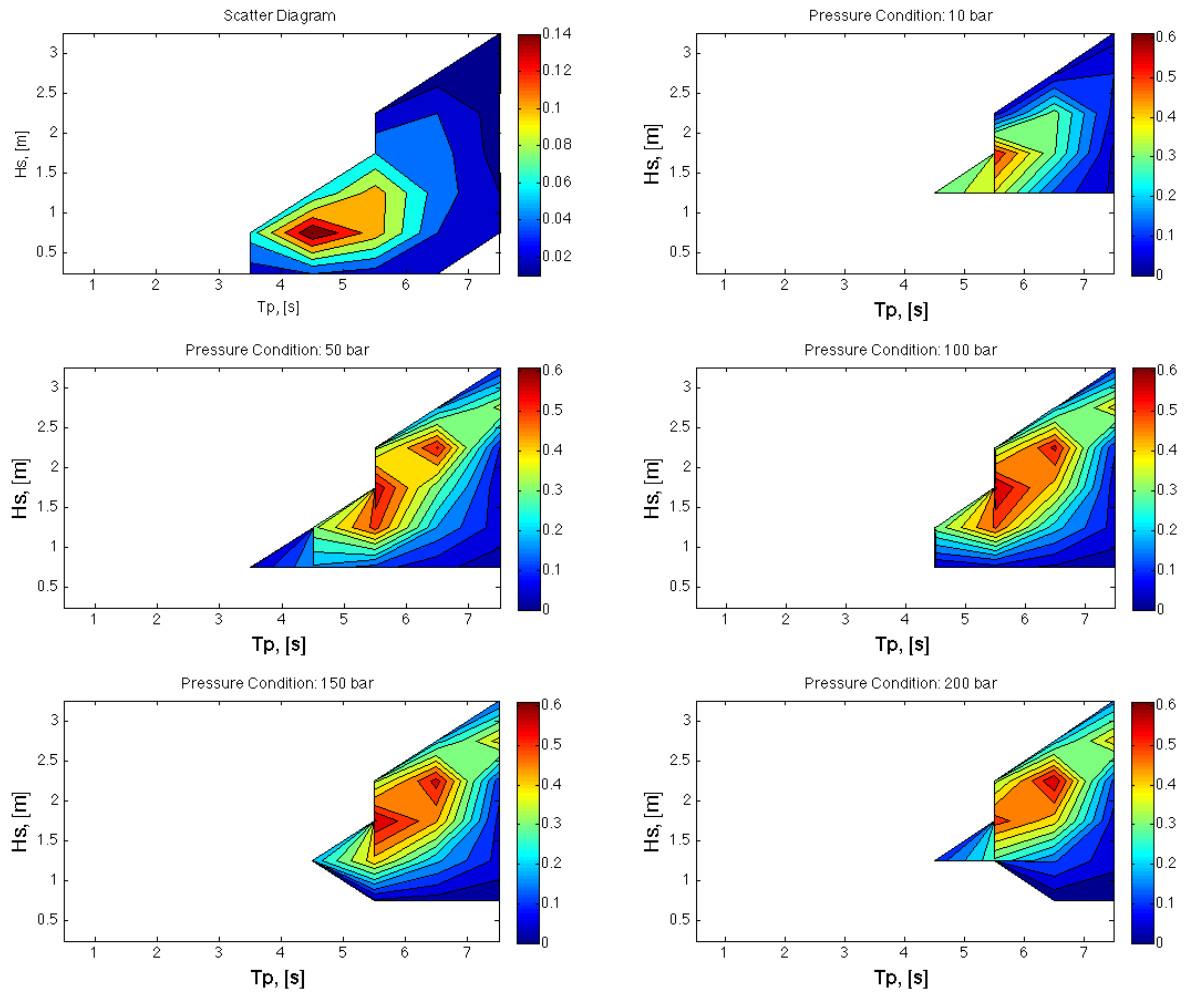

Figure 7.1: Annual power matrix of the simulated scatter diagram for each pressure condition. The top-left figure represents the scatter diagram of the selected loaction. The color map is defined by the probability of occurrence. The other five plots report the annual power matrix, and their color map is the power produced times the related probability in kW. White areas represent condition with negligible power poroduction
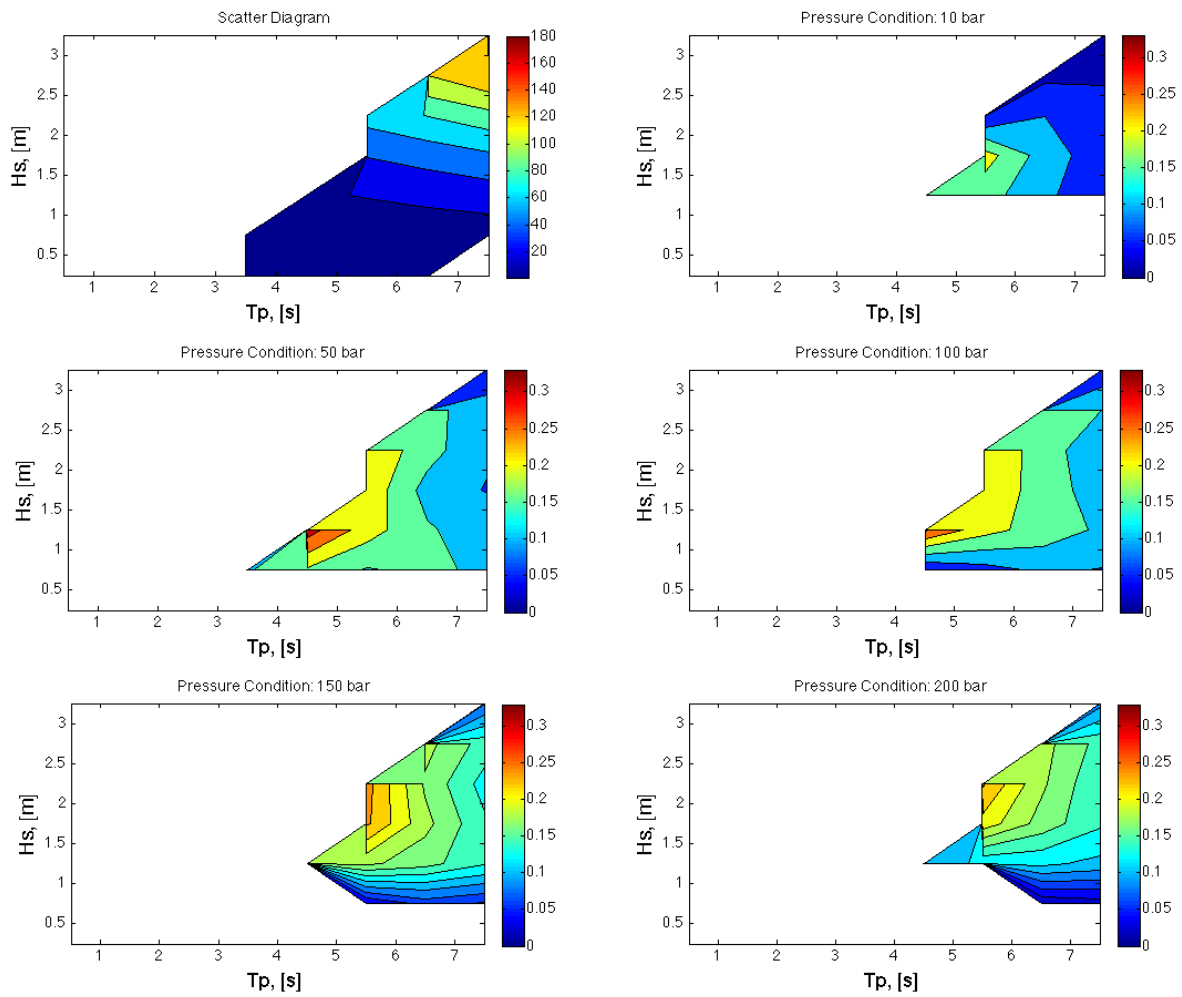
Figure 7.2: Mean efficiencies for the simulated scatter diagram for each pressure condition. The top-left figure reports the incoming wave power in kW. The other five plots report the efficiency of the device in function of the wave state in %. White areas represent condition with negligible power poroduction

in the relative subtitle.

Figure 7.1 reports the annual power production matrix for all the tested conditions. In Fig. 7.1, position 1x1 is occupied by the scatter diagram of the considered location, while the other five plots report the annual power production matrix. At a first glance it is possible to notice a relative wide white area in the scatter diagram, caused by the absence of energy at those particular H/T pairs, and an even bigger white area for the power matrix. This is

mainly linked to the level of pressure set-up in the simulation, which prevent the system to move. Literally the hydraulic PTO system induce a modification of the dynamical model of the floater and contrain the system to move when the incoming energy is not sufficient to overcome the energy level at the HP reservoir. The scatter diagram shows a peak at Tp = 5.5s and Hs = 1 m, which coincides with the natural period of the WEC simulated. De facto, during the design process the device was geometrically and structurally defined to match the predominant wave condition al thespecific location. As expected from the considerations above, the highest power production typically happens at periods close to 5.5 s, with a secondary peak located at 6.5 s. The nature of this secondary peak needs to be further investigated.

If we consider only one pressure level, the maximum annual production is achieved at the pressure stage 2 or 3. At the lower pressure stage, the volume of the HP accumulator, the set-point pressure of the relief valve and the hydraulic motor characteristics bound the power production. In fact due to the reduced PTO feedback force, the motion of the floater is higher, which induces a high flow rate pumped from the hydraulic piston to the HP accumulator, which is higher than the motor flow rate. In general at the lower pressure stage the volumetric design of the accumulator and motor seem to be not appropriate. It is important to bear in mind that there was no optimization of the proposed design, which should be a trade-off in order to achieve the best overall efficiency.

At pressure stage 4 and 5 the overall power production is slightly reduce, because the highest power density is balanced by the smaller working area. This behavior is directly linked to the increased PTO feedback force, which constrains the system motion.

Fig. 7.2 reports the efficiency of the tested case, calculated as the ratio between the produced electrical power and the incoming wave power. This last is a function of the pair H/T and the device length. In Figure 7.2 position 1x1 is occupied by the incoming wave power matrix. The efficiency of the system is somewhere around 0.2 and 0.35 in all the tested cases, inline with the efficiency measured on the real device, deployed in Hanstholm. The highest value is observable at pressure stage 2 and 3, for a peak wave period around 5 s. Also in this case, stage 1, 4 and 5 seems to be a non-optimal global solution.

It is worth to collect the highest value for each sea state into a global picture, Fig. 7.3. In general this is true if we assume the presence of a controller into the HP accumulator. The task of this controller is to slowly change the pressure into the HP reservoir in accordance with the incoming sea state. The controller period will be somewhere around 1-3h. The controlled variable should be the motor speed or its swept volume.

Fig. 7.3 shows an hypotethic optimal annual power matrix. Comparing the annual power production for each of the tested pressure stage, with the overall matrix an improvement of 10% can be achieved.

All the results reported above are related to the electrical power production. Therefore,
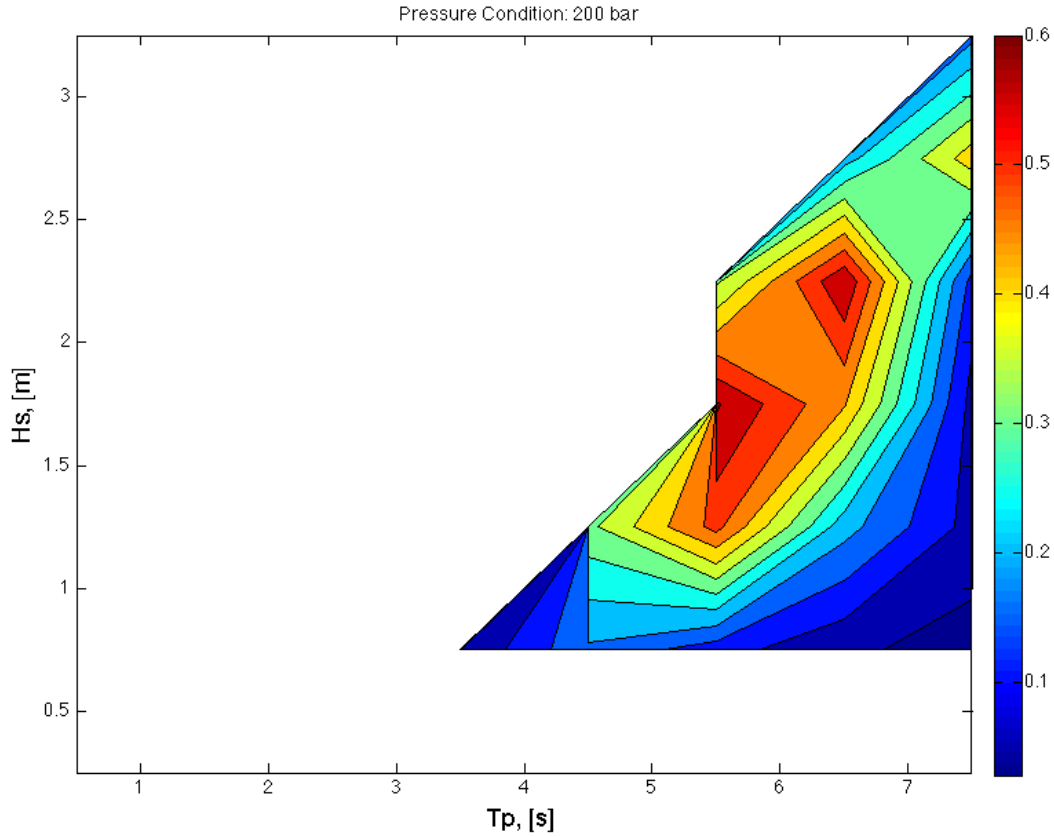
Figure 7.3: Optimal annual power matrix for the simulated scatter diagram. White areas represent condition with negligible power poroduction

it is worth to understand the presence of any bottleneck/point of losses in the transformation chains, which goes from the incoming wave power to the electrical generated power. For this purpose, the power have been assessed at three different locations:

- absorbed power at the floater

- accumulated power into the HP accumulator

- electrical power at the generator

Table 7 reports the efficiency ordered as follow: in the rows, the different wave states, with the relative pair H/T, and in the columns, the pressure levels tested. For each pressure level, the three different efficiencies, introduced above, are listed. A color map between low (0%, green) and high (35%, red) efficiency value is used. The results summarized in Table 7 can be recapped in three points:

(Hs/Tp)	deltaP	deltaP1			deltaP2			deltaP3			deltaP4			deltaP5		
		Pabs	Pacc	Pel	Pabs	Pacc	Pel	Pabs	Pacc	Pel	Pabs	Pacc	Pel	Pabs	Pacc	Pel
		eff, [%]			eff, [%]			eff, [%]			eff, [%]			eff, [%]		
(0.25 / 3.5) ws1		18.4	19.2	0.0	5.4	5.5	0.0	0.0	0.0	0.0	0.0	0.0	0.0	0.0	0.0	0.0
(0.25 / 4.5) ws2		16.2	16.8	0.0	7.5	7.6	0.0	0.1	0.1	0.0	0.0	0.0	0.0	0.0	0.0	0.0
(0.25 / 5.5) ws3		13.8	14.4	0.0	8.4	8.5	0.0	0.6	0.6	0.0	0.0	0.0	0.0	0.0	0.0	0.0
(0.25 / 6.5) ws4		12.8	13.3	0.0	9.5	9.7	0.0	1.0	1.0	0.0	0.0	0.0	0.0	0.0	0.0	0.0
(0.75 / 3.5) ws5		4.9	5.0	0.0	17.8	17.9	14.9	6.6	6.6	0.0	3.5	3.5	0.0	1.2	1.2	0.0
(0.75 / 4.5) ws6		4.0	4.0	0.0	20.6	20.8	18.9	6.2	6.3	0.0	4.0	4.0	0.0	1.7	1.7	0.0
(0.75 / 5.5) ws7		3.5	3.6	0.0	19.7	19.9	15.0	6.2	6.2	0.0	6.0	6.0	4.1	2.6	2.6	0.0
(0.75 / 6.5) ws8		3.2	3.3	0.0	18.3	18.5	17.0	6.4	6.4	0.0	8.5	8.5	7.2	3.8	3.8	2.7
(0.75 / 7.5) ws9		2.8	2.8	0.0	15.0	15.1	13.7	5.6	5.6	0.0	9.0	9.0	6.2	3.5	3.5	3.2
(1.25 / 4.5) ws10		30.6	31.0	29.6	33.4	33.7	32.5	16.7	16.7	14.8	23.0	23.0	20.6	14.7	14.6	11.2
(1.25 / 5.5) ws11		17.7	18.0	17.1	22.4	22.7	22.1	16.3	16.3	12.4	20.7	20.7	18.4	14.7	14.7	12.3
(1.25 / 6.5) ws12		11.2	11.4	10.7	16.9	17.0	15.6	16.3	16.3	15.0	18.7	18.6	16.8	15.3	15.2	12.3
(1.25 / 7.5) ws13		7.4	7.5	6.9	12.9	13.0	12.3	14.4	14.4	13.4	16.3	16.3	14.2	14.7	14.7	11.4
(1.75 / 5.5) ws14		22.9	23.0	21.9	24.4	24.5	23.7	24.4	24.5	23.9	25.8	25.8	24.5	23.8	23.7	21.1
(1.75 / 6.5) ws15		12.9	13.0	12.5	13.5	13.7	13.2	18.0	18.0	17.1	19.8	19.8	18.5	19.5	19.4	17.2
(1.75 / 7.5) ws16		7.2	7.3	6.9	10.1	10.2	9.8	14.4	14.4	13.6	15.5	15.5	14.4	16.2	16.2	14.3
(2.25 / 5.5) ws17		7.7	7.9	5.0	25.2	25.2	24.4	25.4	25.3	24.5	25.5	25.4	24.9	25.4	25.3	24.3
(2.25 / 6.5) ws18		11.4	11.5	9.9	17.8	17.8	17.1	18.1	18.1	17.4	18.1	18.1	17.7	19.4	19.4	18.4
(2.25 / 7.5) ws19		9.4	9.4	8.8	10.9	11.0	10.6	11.7	11.7	11.4	13.6	13.6	13.2	15.2	15.2	14.3
(2.75 / 6.5) ws20		5.4	5.5	3.8	17.4	17.4	16.0	19.4	19.2	18.6	19.4	19.3	18.7	19.4	19.3	18.8
(2.75 / 7.5) ws21		4.7	4.8	3.6	14.1	14.0	13.1	15.9	15.8	15.2	15.8	15.7	15.2	15.9	15.8	15.4
(3.25 / 7.5) ws22		2.5	2.5	1.5	6.9	6.9	5.2	8.1	8.1	6.0	9.9	9.9	7.9	11.5	11.4	9.5

Table 4: Efficiency loss through the transformation chain. The absorbed power at the floater (Pabs), the accumulated power at the HP reservoir (Pacc) and the electrical power (Pel) are reported for each pressure condition and sea state.

- 65%, at the best, of the incoming energy is lost on the wave-body interface. This result is inline with the result presented by [18]

- The energy transformation from kinetic (floater motion) to pressure (potential accumulated at the HP accumulator) does not induce any losses.

- In the worst case 3% of the accumulated energy is lost in the motor/generator block

A closer look at the data reveals that in some case the accumulated power overtake the absorbed power, by 0.1%. This result can be mainly addressed to the simulation inaccuracy related to the highly non-linear system of equations. In particular the fluid compressibility causes high frequency oscillation that are cut by the simulation step width. The results above are strongly correlated to the PTO characteristics summarized in Table 3. For example, the ratio between leakage and maximum area of the check valve is 1e-9, which entails no backward flux and no energy loss in the valve stage. The pipe connections and valves losses are considered negligible, but they can be simulated using a lumped model as reported in [5]. It is important to bear in mind that, the PTO design optimization was not the scope of this work.

As introduce above, the dynamical model of the floater is highly affected by the presence of the hydraulic PTO system. Fig. 7.4 shows the power spectral density trends for ws14 and pressure stage 2. The lines represent the normalized power spectral density (PSD) of the

angular acceleration, velocity and position, the surface elevation, and the radiation, restoring and PTO moments. The normalization was used only for graphical reasons. A zoomed view is also given in the plot area, in order to emphasize the secondary dynamic. The effect
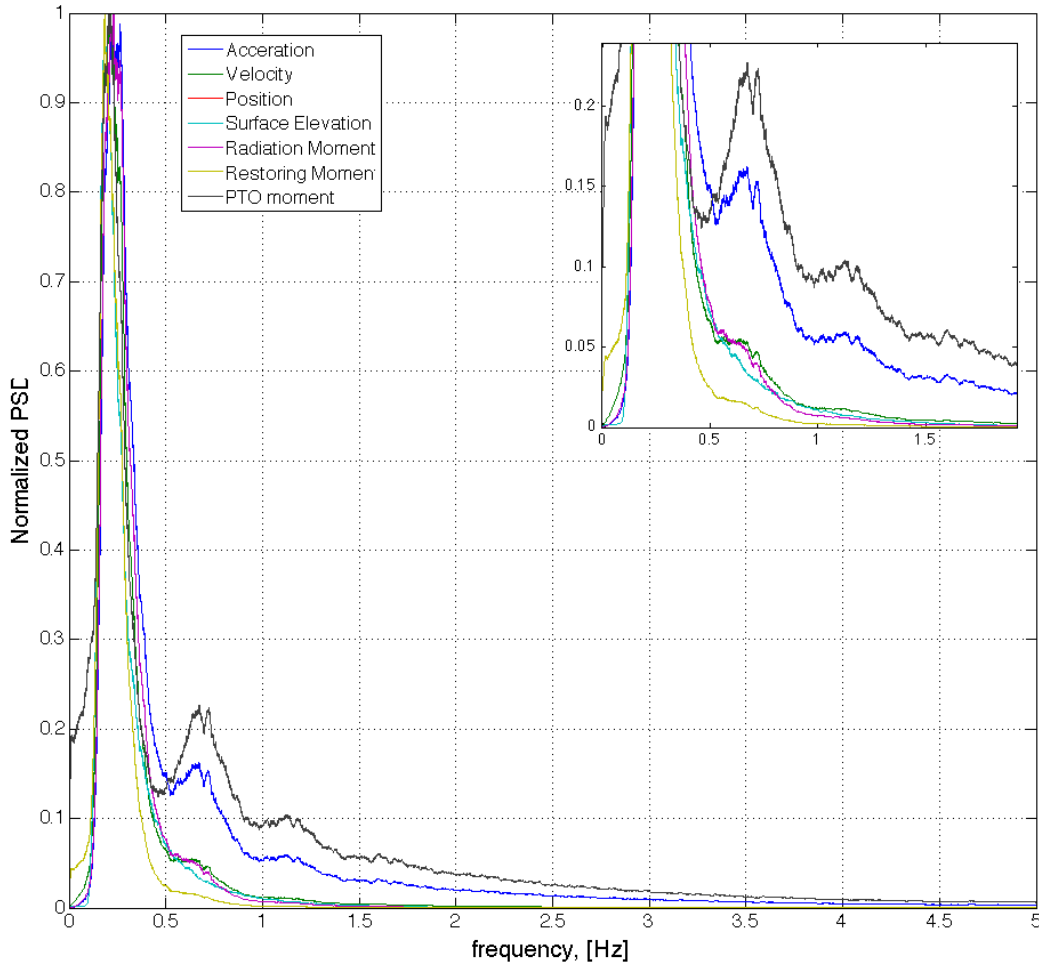

Figure 7.4: Normalized power spectral density (PSD) of the time series relative to ws14 and pressure stage 2. The zoomed view represent the low frequency range.

depicted in Fig. 7.4 highlights the influence of the PTO dynamic on the system, which is mainly caused by the stiffness of the PTO. This last is affected by the fluid compressibility, check valves dynamic, pressure level at the accumulator, gas compressibility, etc., and changes in time. The main effect is visible in the acceleration signal and it can create fatigue problem on the structure.

Since the utilization of an hydraulic PTO with accumulator is mainly related to the reduction of the generated power pulsation, some important consideration can be extracted from the evolution in time of the HP accumulator pressure and the generated power. Fig. 7.5 shows the time evolution of the HP accumulator pressure for five different sea state and Fig. 7.6 shows the generated power for the same conditions. All the conditions reported are at the pressure stage 2 (50 bar). From a general point of view it is possible to find the best match,
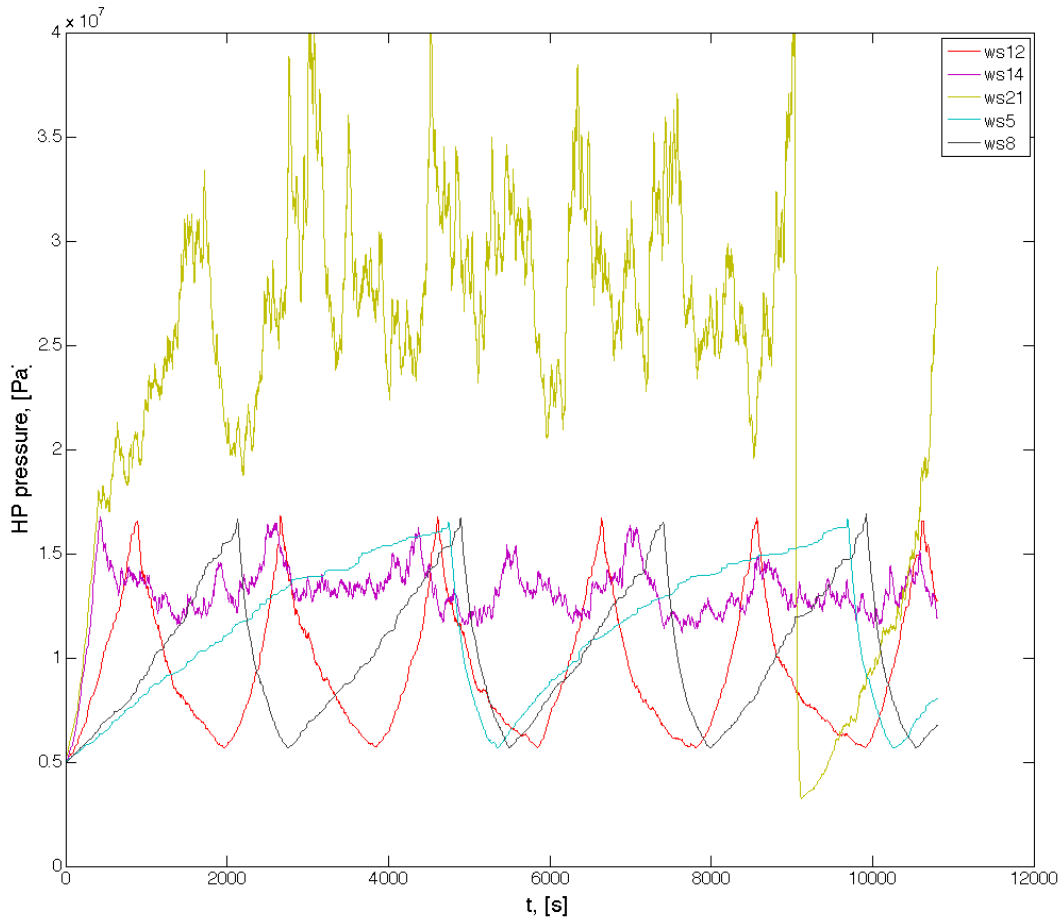
Figure 7.5: Time evolution of the istantanous pressure at the HP accumulator for five sea states. Color lines specification is given in the legend

between PTO configuration and sea state, somewhere around ws12 and ws14, see Table 7 for the sea state specification. At lower sea states, such as ws5 and ws8, the hydraulic motor seems to be over-sized, causing an unwanted power pulsation. In fact the energy take more
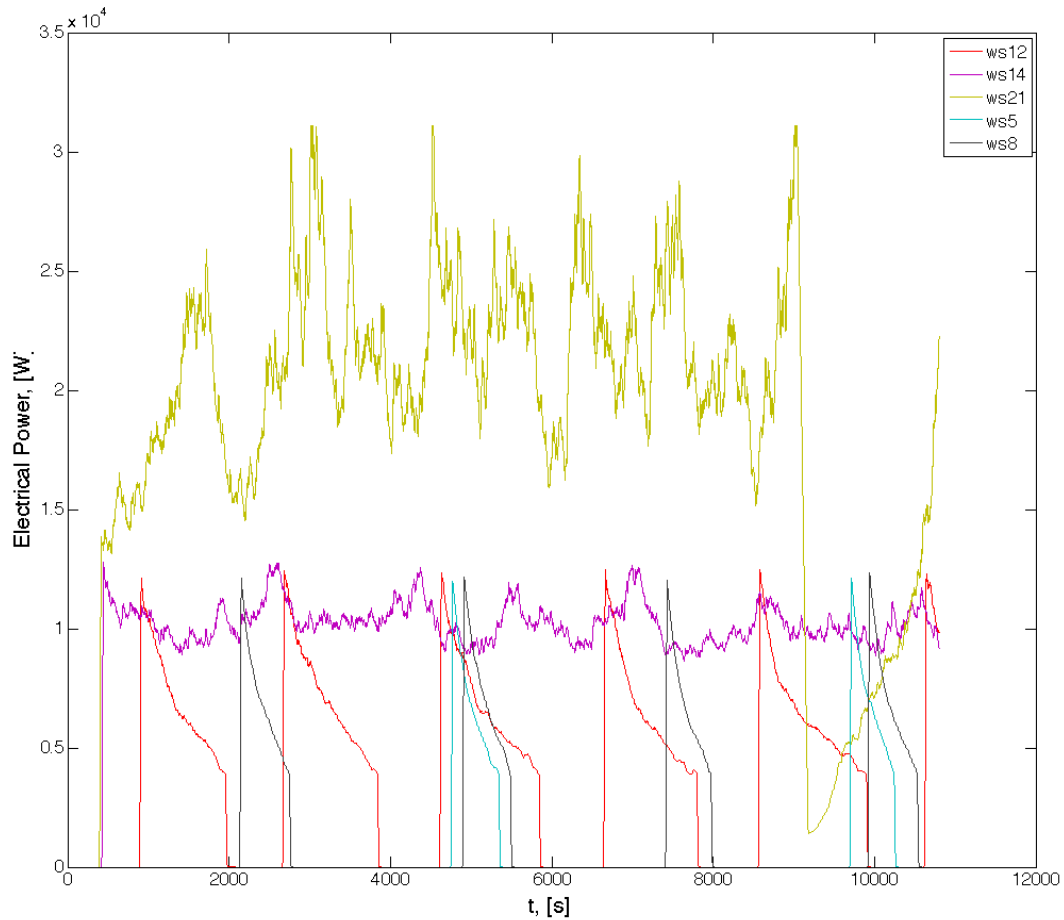
Figure 7.6: Time evolution of the instantaneous electrical power for five sea states. Color lines specification is given in the legend

time to build-up than the time required to be consumed. On the contrary, for higher sea state, such as ws21, the motor seems to be under-sized, which cause the pressure to reach the relief valve set point. This event can be clearly seen in Fig. 7.5 at time 900s. The relief valve is set in such a way that the initial pressure condition is restored when the valve open, in order to avoid the so-called chattering, which in turn cause the simulation to slow down. The fixed displacement motor allows the best performance only in the intermediate sea states. In this range the generated power pulsation is highly reduced, compared with the absorbed power. The behavior of ws12 still presents pulsations, but the time band for the motor is on condition, is higher than the motor-off one. An improvement of the electrical power generation can be achieved in this case by simply changing the motor/generator control ar-

chitecture. In general both the figures shows the need of increase the system flexibility, in order to enlarge the match between incoming energy and absorbable energy. Either changing the PTO architecture or adding a variable displacement motor can do this. Another way to increase the system efficiency is to allow the motor speed to change, because the generator with FC can meanage speed variations. On the other hand changing the fixed displacement motor size it is not a solution, because it will only change the working range position, and not its area.

8　Conclusion

The present report gave a general overview of the hydraulic PTO systems. Nowadays, the interest on this type of systems for applications in the wave energy field is mainly related to the lack of a real/reliable alternative to convert the absorbed power into electricity. In fact, the principle of avoiding prototype on prototypes, defines the need of a well vaidated PTO technology. Hydraulic PTO systems are extensivelly studied, because they are robust and their features match the wave energy ones, i.e. low period and high loads. Different hydraulic PTO architectures have already been studied in the last year. In this specific work, type 1 has been implemented. The system is composed by a double action hydraulic piston, a rectifying bridge of check-valves, a HP and LP accumulators, a hydraulic fixed displacement motor and a generator. The fluid compressibility is implemented using the fluid bulk modulus. The model implemented shows different limitations, i.e. poor flexibility with respect to the incoming sea state, even if this was not the scope of the work, which cause the system to be far away from its optimal configuration. In any case the performance of the model are in line with the Wavestar prototype installed in the Nord Sea. This type of PTO system induces a deep modification of the hydrodynamic model, causing motion constrains, fast and secondary dynamics, and high loads on the floater arm.

References

[1] R. Henderson, "Design, simulation and testing of a novel hydraulic power take-off system for the pelamis wave energy converter," *Renewable Energy*, vol. 31, pp. 271–283, 2006.

[2] J. Lasa, J. C. Antolin, C. Angulo, P. Estensoro, M. Santos, and P. Ricci, "Desing, construction and testing of a hydraulic power take-off for wave energy converters," *Energies*, vol. 5, pp. 2030–2052, 2012.

[3] Y. Kamizuru, L. Verdegem, P. Erhart, C. Langenstein, L. Andren, M. LenBen, and H. Murrenhoff, "Efficient power take-offs for ocean energy conversion," in *ICOE*, (Dublin), 2012.

[4] A. F. d. O. Falcao, "Modelling and controll of oscillating-body wave energy converters with hydraulic power take-off and gas accumulator," *Ocean Engineerign*, vol. 34, pp. 2021–2032, 2007.

[5] K. Schlemmer, F. Fuchsumer, N. Boemer, R. Costello, and C. Villegas, "Design and controll of a hydraulic power take-off for an axi-symmetric heaving point absorber," in *EWTEC*, (Southampton), 2011.

[6] J. Hals, R. Taghipour, and T. Moan, "Dynamics of a force-compensated two-body wave energy converter in heave with hydraulic power take-off subject to phase control," in *EWTEC*, (Porto), 2007.

[7] H. Eidsmoen, "Simulation od a slack-moored heaving-buoy wave-energy converter with phase control," 1996.

[8] H. Eidsmoen, "Simulation od a tight-moored amplitude-limited heaving-buoy wave-energy converter with phase control," 1996.

[9] C. Josset, A. Babarit, and A. H. Clement, "A wave-to-wire model of the searev wave energy converter," *Journal of Enginnering for the Maritime Environment*, vol. 81, 2007.

[10] R. Costello, J. V. Tingwood, and J. Weber, "Comparison of two alternative hydraulic pto concepts for wave energy conversion," in *EWTEC*, (Southampton), 2011.

[11] Y. Kamizuru, M. Lermann, and H. Murrenhoff, "Simulation of an ocena wave energy converter using hydraulic transmission," in *International Fluid Power Conference*, (Aachen), 2010.

[12] A. F. d. O. Falcao, P. A. P. Justino, J. C. C. Henriques, and J. M. C. S. Andre, "Reactive versus latching phase control of a two-body heaveing wave energy converter," 2008.

[13] G. Bacelli and J. V. Ringwood, "A control system for a self-reacting point absorber wave energy converter subject to constrains," in *IFAC*, (Milan), 2011.

[14] P. Ricci, J. Lopez, M. Santos, J. L. Villate, P. Ruiz-Minguela, F. Salcedo, and A. F. d. O. Falcao, "Control strategy for a simple point absorber connected to a hydraulic power take-off," in *EWTEC*, (Uppsala), 2009.

[15] W. E. Cummins, "The impulse response function and ship motion," in *Symposium on Ship Theory*, (Hamburg), 1962.

[16] H. E. Merrit, *Hydraulic control system*. New York: John Wiley and Sons, 1967.

[17] P. Frigaard, M. Hogedal, and C. M, *Wave generation theory*. Aalborg: Aalborg University, 1993.

[18] M. M. Kramer, L. Marquis, and P. Frigaard, "Performance evaluation of the wavestar prototype," in *EWTEC*, (Southempton), 2011.

Appendices

A   Wavestar: Hydrodynamic and hydrostatic parameters

Moment of Inertia (J): $[kgm^2]$
$2.45*10^6$

Hydrostatic Restoring Moment (kh): [Nm/rad]
$14.0*10^6$
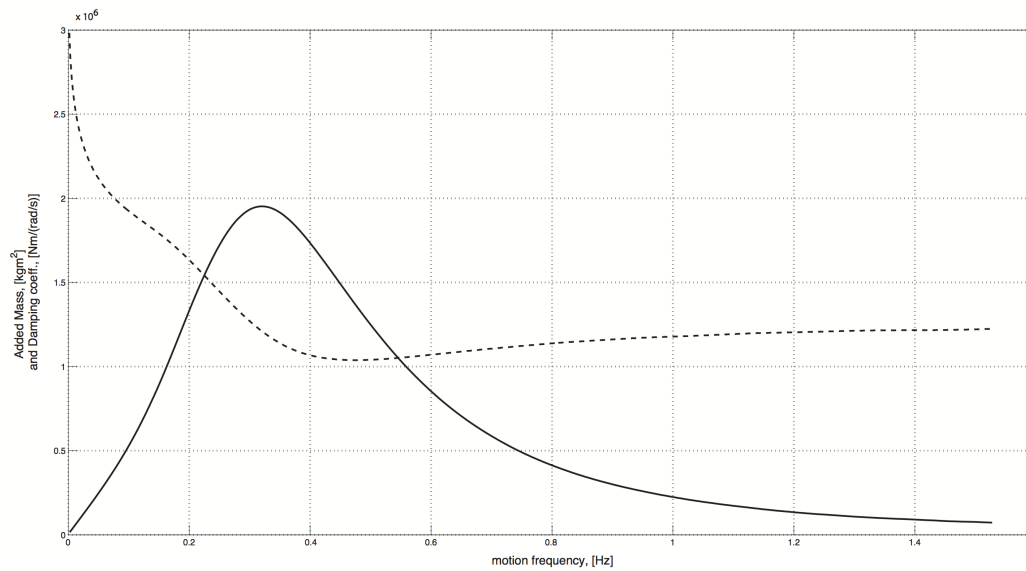
Figure A.1: Radiation moment frequency response function: Damping (full draw line) and Added Mass (dotted line) in function of the frequency of the motion
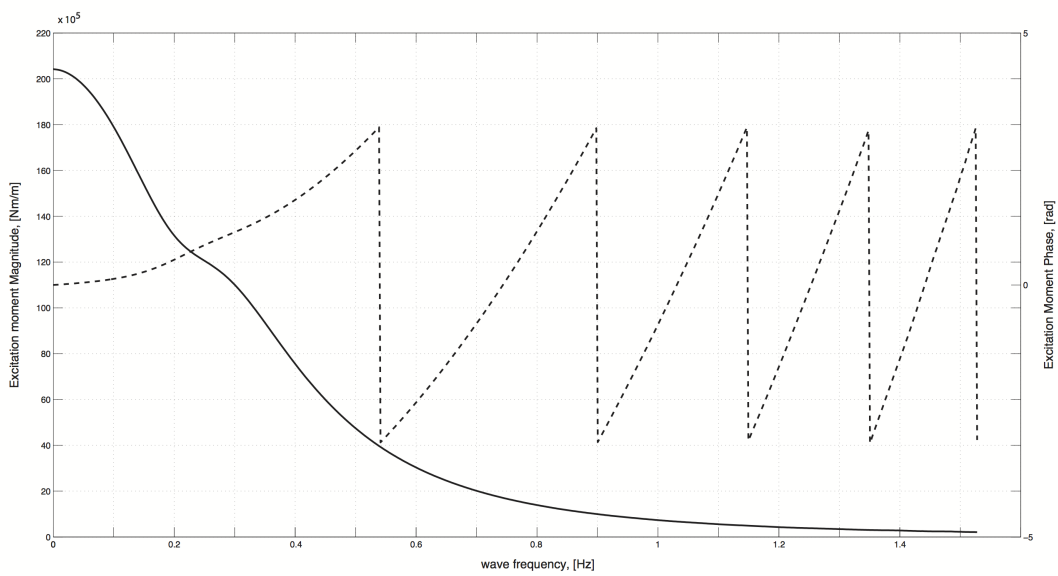
Figure A.2: Excitation moment frequency response function: Magnitude (full draw line) and Phase (dotted line) in function of the frequency of the incoming waves

B PTO length

α is the angle in A, which can be obtained from the angular displacement θ
γ is the angle in C
β is the angle in B

$$\overline{BC} = \sqrt{\overline{AB}^2 + \overline{AC}^2 - 2\overline{AB} \cdot \overline{AC} \cdot cos(\alpha)}$$

$$K = sin(\alpha) \cdot \frac{\overline{AB} \cdot \overline{AC}}{\overline{BC}}$$

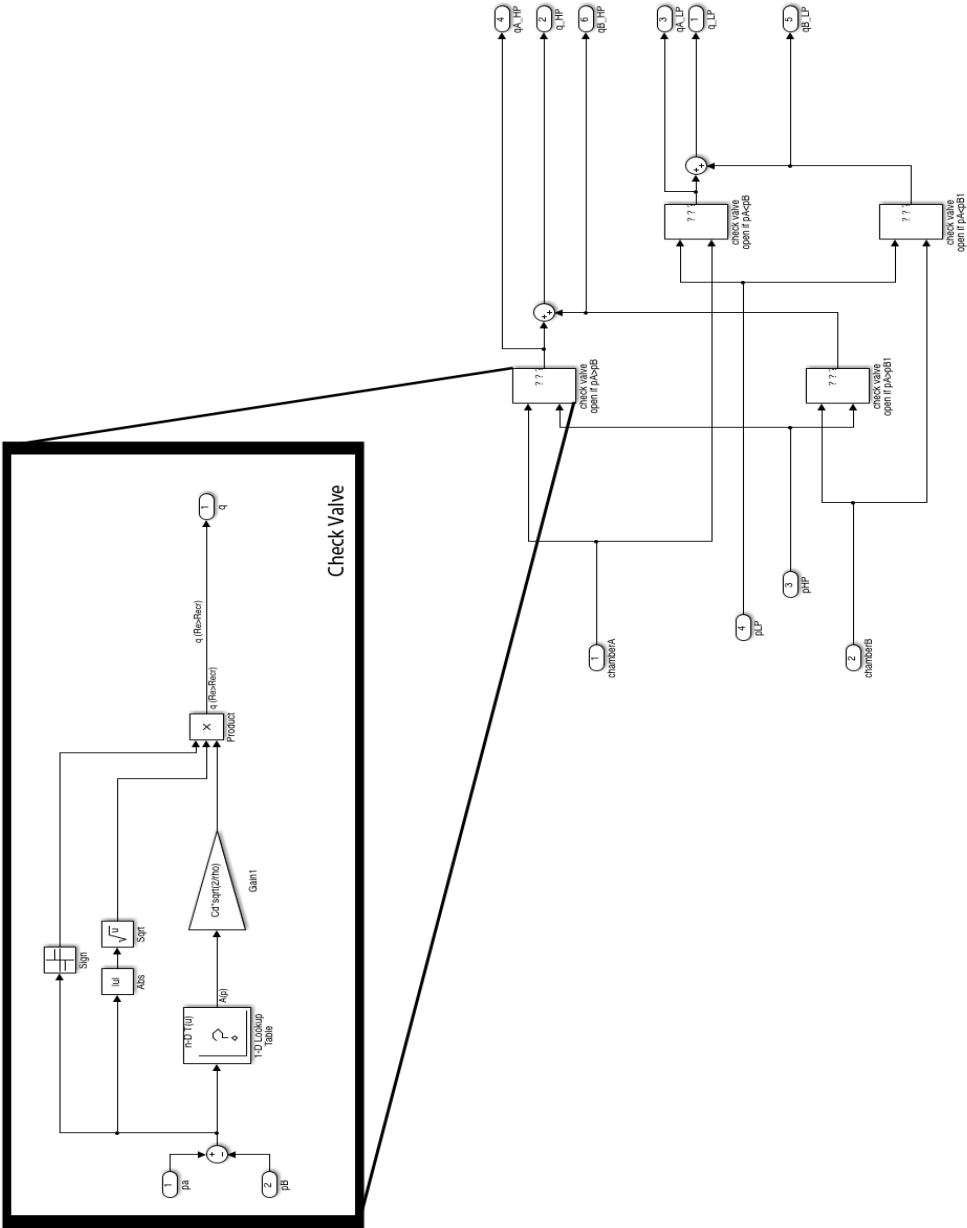K is the moment arm

C   Simulink Model

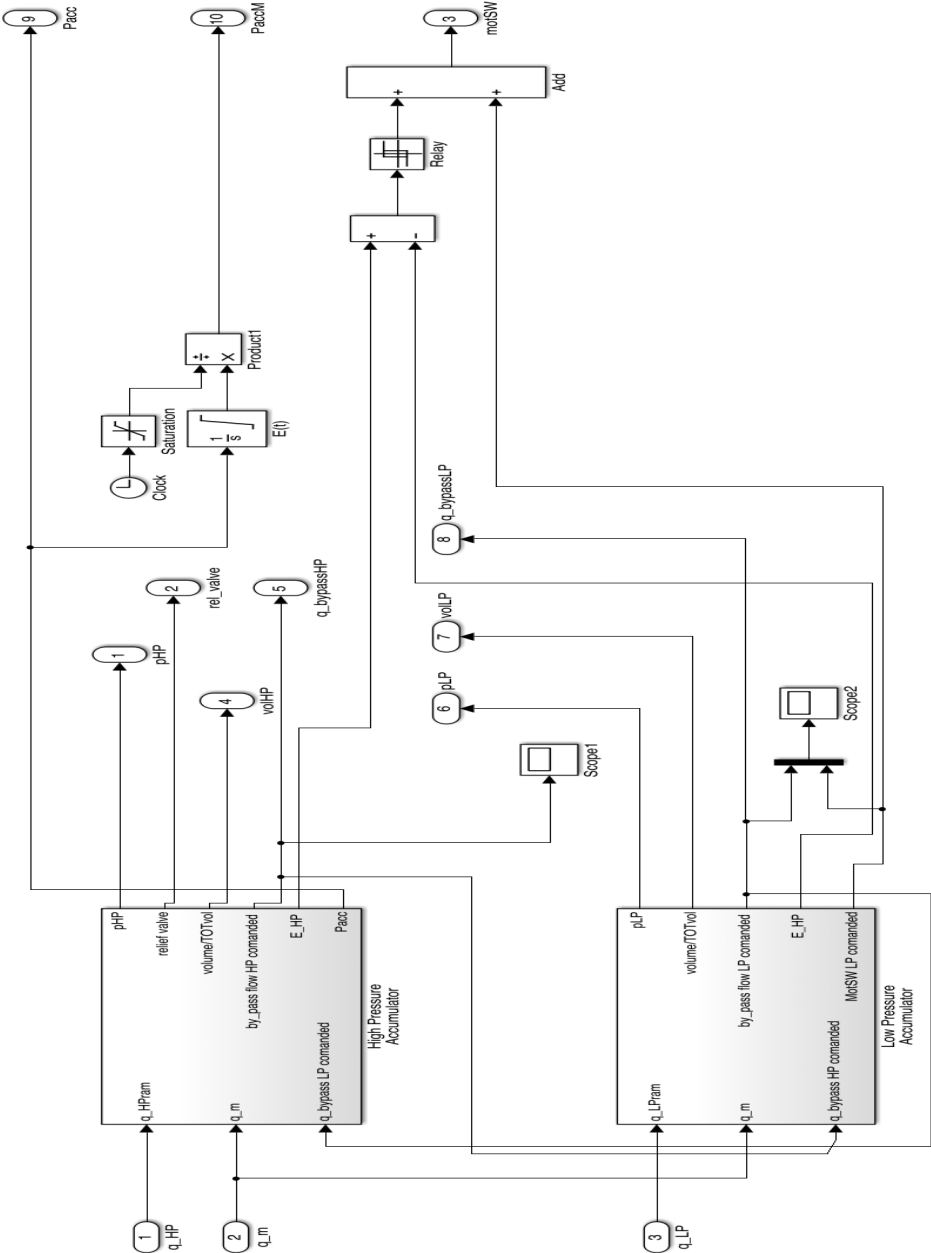## C.1   Simulink Submodels: Floater
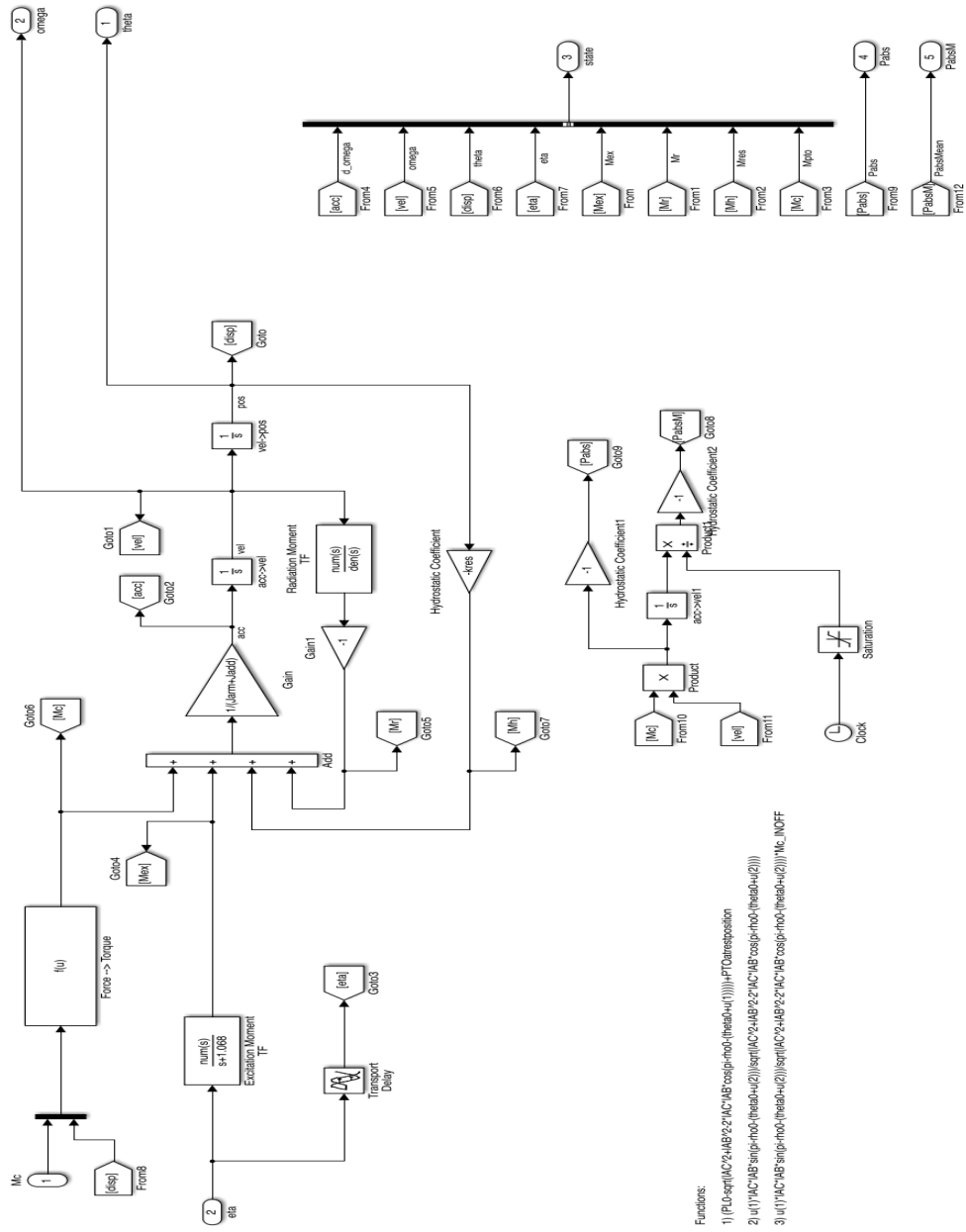
C.2 Simulink Submodels: Hydraulic Piston
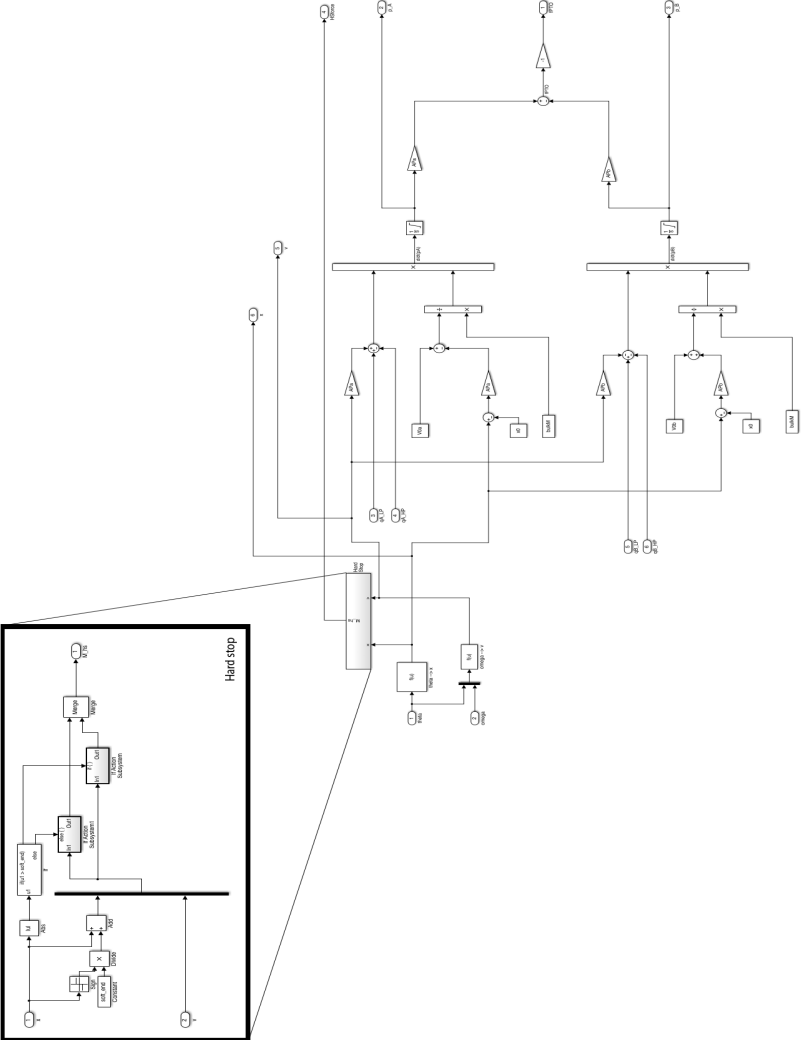
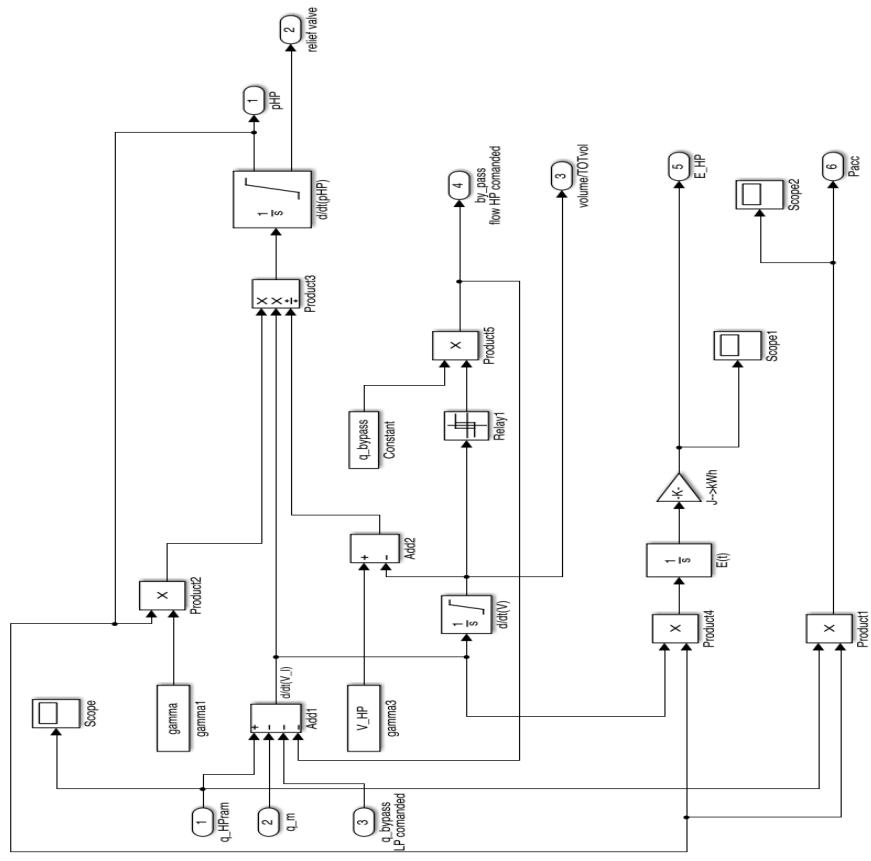## C.3   Simulink Submodels: Check Valves Bridge Rectifier

C.4   Simulink Submodels: HP and LP accumulators

High pressure (HP) reservoir

47

The pressure inside the low pressure resevoir is considered
and equal to the atmospheric pressure

Low pressure (LP) reservoir

C.5 Simulink Submodels: Motor and Generator